Title

Epigenetic targeting of the Nanog pathway and signaling networks during chemical carcinogenesis

Journal

Carcinogenesis, 35(8)

ISSN

0143-3334

Authors

Tommasi, Stella

Zheng, Albert

Yoon, Jae-In

et al.

Publication Date

2014-08-01

DOI

10.1093/carcin/bgu026

Peer reviewed

Carcinogenesis vol.35 no.8 pp.1726–1736, 2014
doi:10.1093/carcin/bgu026
Advance Access publication January 30, 2014

Epigenetic targeting of the *Nanog* pathway and signaling networks during chemical carcinogenesis

Stella Tommasi, Albert Zheng, Jae-In Yoon[1] and Ahmad Besaratinia*

Department of Preventive Medicine, Keck School of Medicine of USC, University of Southern California, M/C 9603, Los Angeles, CA 90033, USA and [1]QIAGEN, 1012 C Bldg, Woolim-Lions Valley, 371-28 Gasandong, Gumchungu, Seoul, Republic of Korea

*To whom correspondence should be addressed. Tel: +1 323 442 7251; Fax: +1 323 865 0103;
Email: besarati@med.usc.edu

Chemical carcinogenesis has long been synonymous with genotoxicity, which entails DNA damage, genetic mutations and chromosomal abnormalities. The present study investigates a paradigm-shifting model in which epigenetic changes are key contributors to chemical carcinogenesis. Using genome-wide microarray-based analysis followed by conventional validation assays, we have progressively chronicled changes in the epigenetic landscape, as reflected in the patterns of DNA methylation, in the target organ of tumorigenesis in mice treated *in vivo* with a prototype chemical carcinogen (benzo[a]pyrene). Here, we demonstrate characteristic CpG island gain/loss of methylation and demethylation of repetitive DNA elements in carcinogen-treated mice, dependent on tumor progression. Alterations of the DNA methylome are accompanied by silencing of major DNA methyltransferases. Members of the *Nanog* pathway that establishes and maintains pluripotency in embryonic stem cells and possibly triggers uncontrolled proliferation of neoplastic cells are preferential targets of aberrant DNA methylation and concomitant gene dysregulation during chemical carcinogenesis. Several components of the *MEK/ERK*, *JAK/STAT3*, *PI3K/AKT*, *WNT/β-catenin* and *Shh* signaling cascades, which are known to modulate *Nanog* expression, also show concurrent changes in the patterns of DNA methylation and gene expression. Our data support an epigenetic model of chemical carcinogenesis and suggest that surveillance of the epigenetic landscape, particularly at the loci and in the pathways identified in this study, may have utility for early detection and monitoring of the progression of malignancy.

Introduction

Chemical carcinogenesis has long been ascribed to genotoxic events, which entail DNA damage, genetic mutations and chromosomal abnormalities (1–3). In addition to genotoxicity, chemical carcinogens may also possess a non-genotoxic mode of action, e.g. epigenetic effects, which are emerging as key contributors to carcinogenesis (4–6). Epigenetic effects include aberrant DNA methylation, histone modifications and variants, miRNAs dysregulation, chromatin remodeling and nucleosome positioning (7–9). Of these, aberrant DNA methylation is the most extensively studied epigenetic alteration in carcinogenesis (7,8). Gain of methylation (hypermethylation) at CpG islands, clustered at the promoter, 5′-untranslated region and exon 1 of known genes (promoter CpG islands) or localized within gene bodies (intragenic CpG islands) is a common event in cancer (9–11). Global loss of methylation (hypomethylation) at repetitive DNA elements, such as long and short interspersed nuclear elements (LINEs and SINEs, respectively), and long terminal repeat (LTR) retrotransposons is also a frequent occurrence in carcinogenesis (12–14).

Although human population studies and animal model experiments have established an association between exposure to chemical carcinogens and epigenetic effects, a direct cause and effect relationship has yet to be established (4,5). Suggestive evidence exists in support of a causal link between epigenetic effects and chemical carcinogenesis. For example, the reactive metabolite of a prototypical chemical carcinogen, benzo[a]pyrene (B[a]P) (15), binds preferentially to methylated CpG sites (16), thereby, possibly impeding the establishment and/or maintenance of DNA methylation patterns by DNA methyltransferases (DNMTs) and methyl-CpG-binding domain (MBDs) proteins (17–19). It is also plausible that carcinogen-induced DNA damage may cause mutations in genes maintaining the epigenetic state, including those regulating the DNA methylation machinery and chromatin-modifying enzymes (20,21).

The objectives of the present study were 2-fold: (i) to investigate whether epigenetic effects occur in response to exposure to chemical carcinogens and, if so, (ii) to determine whether epigenetic effects are predictors of chemically induced carcinogenesis. To attain these objectives, we have performed genome-wide DNA methylation analysis in the target organ of tumorigenesis, i.e. seminal vesicles, in mice treated *in vivo* with B[a]P both before and after tumor development. For verification purposes, we have confirmed the data obtained by our genome-wide microarray-based analysis (22) using the conventional single-gene methylation detection assays (23,24). Furthermore, we have used a bisulfite sequencing-based assay (25) to determine the methylation status of major repetitive DNA elements, including LINE L1, intracisternal A particle (IAP) LTR and SINE B1 (26–28), in B[a]P-treated mice both before and after tumor development. Here, we demonstrate a relationship between carcinogen exposure, alterations of the epigenome and gene expression changes, particularly in the *Nanog* and its interconnected signaling pathways. Our data indicate that carcinogen exposure results in epigenetic modifications, specifically at loci that control key signaling pathways required for normal cell proliferation during development.

Materials and methods

B[a]P treatment of mice

Thirty adult male mice (6–8 weeks old) on a C57BL/6 genetic background (Stratagene, La Jolla, CA) were randomly divided into two groups: (i) experimental (B[a]P treatment; $n = 15$) and (ii) control (solvent treatment; $n = 15$), each subdivided into three categories, including (i) 6 week treatment (T0), (ii) 6 week treatment + 6 week latency (T1: early lesion formation) and (iii) 6 week treatment + ≥10 week latency (T2: tumor development). A flowchart of the study design is shown in Figure 1A. The mice assigned to each experimental or control group were kept in polypropylene cages in groups of two to three animals per cage and housed in an air-conditioned animal room with controlled ambient temperature, relative humidity and 12 h light/dark cycle. The mice had access to food (PicoLab Rodent Diet 20; PMI Nutrition International, LLC; Brentwood, MO) and water *ad libitum* at all times. All experiments were approved by the Institutional Animal Care and Use Committee in accordance with the recommendations of the National Institutes of Health provided in the Guide for the Care and Use of Laboratory Animals.

The experimental mice received intraperitoneal injections of B[a]P once per week for a duration of 6 weeks using the following protocol: first week: 25 mg/kg body weight (BW); second week: 50 mg/kg BW; third week: 75 mg/kg BW and fourth week to sixth week: 100 mg/kg BW of B[a]P. The specified doses of B[a]P were prepared fresh on the day of administration by dissolving the chemical in dimethyl sulfoxide (DMSO) (B[a]P and DMSO; Sigma–Aldrich, St Louis, MO). The incremental doses of B[a]P were delivered to the mice by intraperitoneal injection (100 µl) on the lower right or left quadrant of the

Abbreviations: B[a]P, benzo[a]pyrene; BW, body weight; COBRA, combined bisulfite restriction analysis; DMSO, dimethyl sulfoxide; DNMT, DNA methyltransferase; ESC, embryonic stem cell; H&E, hematoxylin and eosin; IAP, intracisternal A particle; IPA, Ingenuity Pathway Analysis; LINE, long-interspersed nuclear element; LTR, long terminal repeat; MBD, methyl-CpG-binding domain; MIRA, methylated CpG island recovery assay; qRT–PCR, quantitative real-time PCR; SINE, short interspersed nuclear element.

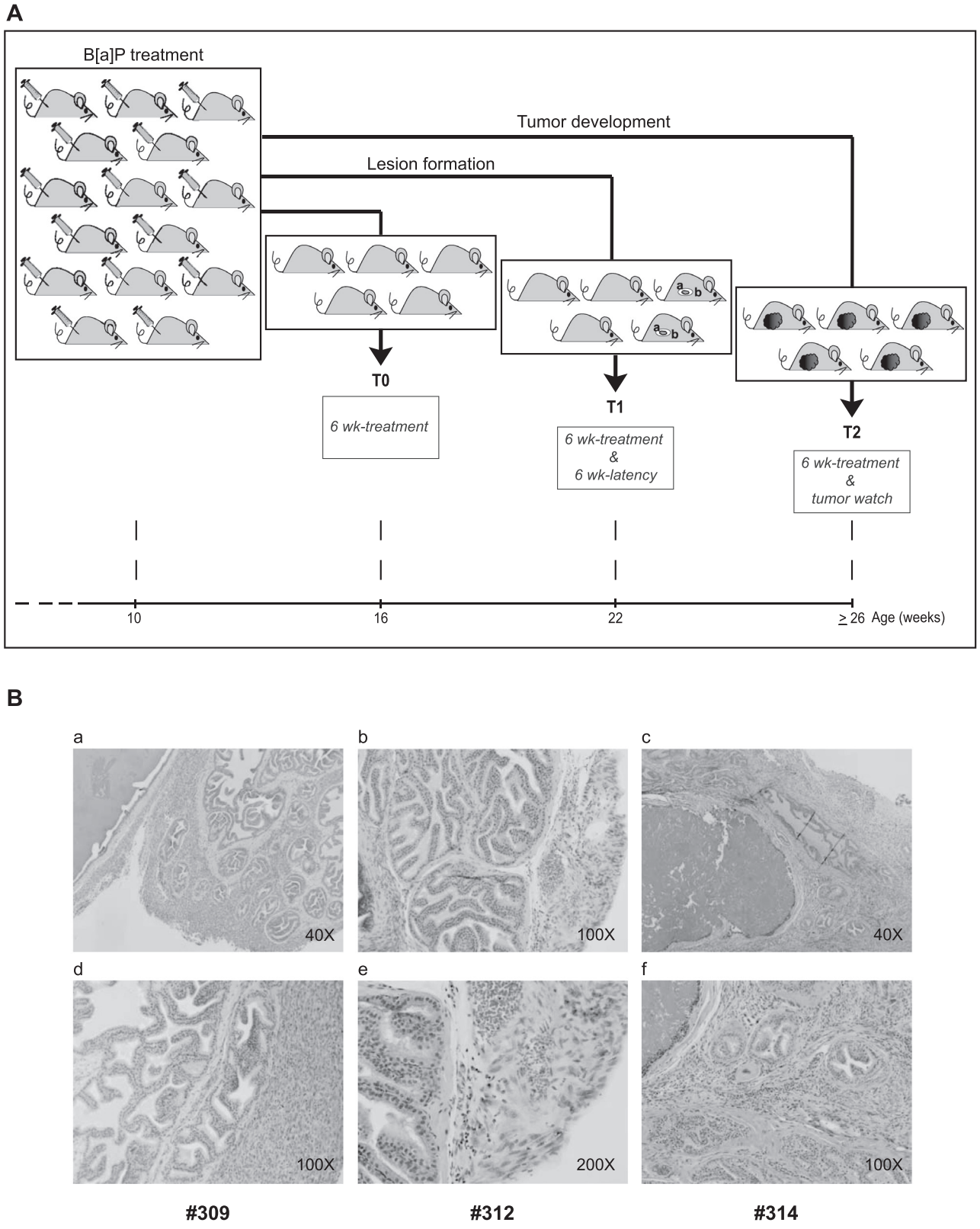

Fig. 1. Outline of the experimental design and histological analysis of tumors in B[a]P-treated mice. (**A**) Adult male mice were treated intraperitoneally with weekly doses of B[a]P over a period of 6 weeks. Subgroups of animals were euthanized immediately after the last B[a]P injection and at ensuing intervals posttreatment. Subsequently, the target organ of tumorigenesis (seminal vesicles) were collected for histological and biochemical analyses. Mice treated with solvent DMSO were used as control (a) precursor lesions; (b) adjacent normal tissues. (**B**) Tumors developed in the seminal vesicles of B[a]P-treated mice were collected in formalin and processed for H&E staining. Sections were photographed at lower (panels a–c) and higher (panels d and e) power magnifications.

abdomen in alternate weeks. Control mice received similar injections of solvent DMSO using the same dosing regimen, as described for B[a]P. All mice were monitored closely for development of any unusual symptoms. At the end of all experiments, the B[a]P-treated mice and controls were euthanized by CO_2 asphyxiation and subjected to necropsy and macroscopic examination. For biochemical assays, the accessory sex organs, including seminal vesicles

and prostate glands or tumors, were harvested, snap frozen and preserved at −80°C until further analysis. Alternatively, the harvested tissues or tumors were fixed in formalin, embedded in paraffin and used for hematoxylin and eosin (H&E) slide preparation according to standard protocols.

Genome-wide DNA methylation profiling

We used the methylated CpG island recovery assay (MIRA) in combination with microarray analysis (22) to catalogue the DNA methylation profile, on a genome-wide scale, in the target organ of tumorigenesis, i.e. seminal vesicles, in mice treated *in vivo* with B[a]P both before and after tumor development. As a pull-down assay for enrichment of the methylated CpG content of DNA, the MIRA is based on the ability of the MBD2b protein to bind methylated CpG dinucleotides, while this reaction is enhanced in the presence of MBD3L1 protein (22). Briefly, genomic DNA was isolated from either seminal vesicles or tumors developed at the same organ site and subjected to MIRA enrichment, as described previously (22). Subsequently, the MIRA-enriched DNA and input DNA fractions were amplified by PCR and labeled and hybridized to the Roche NimbleGen Mouse DNA Methylation 3x720K CpG Island Plus RefSeq Promoter Arrays (Roche NimbleGen, Indianapolis, IN). This set of microarrays covers 20 404 RefSeq gene promoters and 15 988 annotated CpG islands of the mouse genome. The raw microarray data were processed and analyzed using a standard bioinformatics approach, as described in ref. (22). The microarray data have been deposited in the National Center for Biotechnology Information Gene Expression Omnibus database (Accession No: GSE41422).

Single-gene DNA methylation analysis by combined bisulfite restriction analysis and bisulfite sequencing

We used the combined bisulfite restriction analysis (COBRA) (24) and sodium bisulfite sequencing (23) to verify the methylation status of individual target loci/genes identified by MIRA-microarray analysis in the target organ of tumorigenesis in B[a]P-treated mice both before and after tumor development. Briefly, 1 µg of genomic DNA was treated with sodium bisulfite using the Qiagen EpiTect kit according to the manufacturer's instructions (Qiagen, Valencia, CA). Subsequently, the bisulfite-treated DNA was assayed by standard COBRA (24) using sets of primers specifically designed for each target CpG island. The primer sequences used for PCR amplification of all the analyzed targets are available upon request. Mouse genomic DNA was methylated *in vitro* with M. SssI CpG methyltransferase (New England Biolabs, Ipswich, MA) and served as positive control. For genomic sequencing, the PCR products obtained after bisulfite conversion of DNA were cloned into the TOPO-TA cloning vector according to the manufacturer's instructions (Invitrogen, Carlsbad, CA). Up to 10 randomly selected clones from each experimental and control group were sequenced using an ABI-3730 DNA Sequencer (ABI Prism; PE Applied BioSystems, Foster City, CA).

DNA methylation analysis in repetitive DNA elements

We used a bisulfite sequencing-based assay (25) to analyze the methylation status of major repetitive DNA elements, including LINE L1, IAP-LTR and SINE B1, in the target organ of tumorigenesis in B[a]P-treated mice both before and after tumor development. The LINE L1, IAP-LTR and SINE B1 comprise 18.78, 3.13 and 2.66%, respectively, of the mouse genome (26–28). The assay is based on sodium bisulfite treatment of the genomic DNA, followed by primer amplification of the consensus sequences of the respective elements and direct sequencing, thereafter (25). Detailed information on the genomic sequence and primer design of the repetitive DNA elements analyzed in the present study is available in ref. (22).

Motif discovery and canonical pathway analysis

Differentially methylated CpG islands were analyzed for shared *de novo* motifs and known transcription factor recognition sites, using Partek® Genomics Suite™ software (Partek® 6.6). Novel motifs of length 6–16 bp were identified based on their highest score (score = log ratio of the probability that the sequence was generated by the motif versus that by background distribution). Binding sites for known transcription factors were selected from the JASPAR database in Partek based on their high probability of occurrence (*P* value). Functional identification of gene networks and canonical pathways analysis were performed using the Ingenuity Pathway Analysis® program (IPA®: v 9.0) and the GO Enrichment Analysis in Partek® Genomics Suite™.

Quantitative real-time PCR

Standard quantitative real-time reverse transcription–PCR (qRT–PCR) was used to determine the level of transcription of individual target genes identified by MIRA-microarray analysis, as described previously (22). Briefly, total RNA was extracted from the seminal vesicles of mice treated *in vivo* with B[a]P both before and after tumor development, using the RNeasy kit (Qiagen). DNase-treated RNA (0.5 µg) was reverse transcribed into cDNA using SuperScript® VILO™ cDNA Synthesis kit (Invitrogen). The mRNA expression level of target genes was determined by qRT–PCR using the EXPRESS SYBR® GreenER™ qPCR SuperMix (Invitrogen) and the CFX96 Touch™ Real-Time PCR detection system (Bio-Rad). All reactions were performed in triplicate and fold changes were determined using the $2^{-\Delta\Delta C_t}$ method (22). The primer sets used for qRT–PCR are listed in Supplementary Table S1, available at *Carcinogenesis* Online.

Results

Mice survival and tumorigenicity

We have treated adult male mice with progressively increasing doses of B[a]P weekly for a duration of 6 weeks, as described in Materials and methods. For control purposes, we have treated counterpart mice with solvent DMSO using the same protocol as described for B[a]P. Subgroups of animals were euthanized immediately after treatment (T0), 6 week posttreatment (T1) or after tumor development (T2), as outlined in Figure 1A. The mice generally well tolerated B[a]P treatment and had a survival rate of >75%, as determined in two independent sets of experiments. All surviving B[a]P-treated mice developed large aggressive tumors in the seminal vesicles as early as 10 week posttreatment. Small lesions and other abnormalities were also detectable in the secondary sex organs of B[a]P-treated mice at T1. Control mice treated with DMSO showed 100% survival at the end of all experiments and were lesion free at all organ sites.

Histological analysis of B[a]P-induced tumors

The accessory sex organs, including the target organ of tumorigenesis, i.e. seminal vesicles, were collected from all B[a]P-treated and control mice at the time of necropsy, fixed in formalin and subjected to H&E staining. Consistent with landmark studies (29), all surviving B[a]P-treated mice developed large solid masses (Δ: 2.5 × 2 × 2 cm) in the seminal vesicles and prostate glands. Histopathological examination identified the tumors as high-grade sarcomas, mostly leiomyosarcoma. Prominent features of the tumors included characteristic spindle-like cells, abundance of apoptotic cells and mitotic figures, as well as areas of pleomorphism and infiltration (Figure 1B, panels a–f). One mouse from group T0 and all mice from group T1 had macroscopic abnormalities in the genitourinary tract. These aberrations often consisted of (uni)-testicular atrophy and/or hyperplasia of seminal vesicles/prostate (mostly on the left side), which are likely to have preceded the tumors developed in older mice. Hyperplasia and other abnormalities were also observed sporadically in the digestive tract of several mice at the end of treatment (T0), and thereafter (T1 and T2). One mouse from group T2 (#313) also developed an aggressive sarcoma on the intestinal wall. Representative H&E sections of tissues/tumors collected from B[a]P-treated mice are shown in Figure 1B, panels a–f.

DNA methylation profiling during B[a]P-induced tumorigenesis

We have used a genome-wide microarray-based approach (22) to detect aberrant DNA methylation in the target organ of tumorigenesis, i.e. seminal vesicles, in mice treated *in vivo* with B[a]P immediately after treatment (T0) and following tumor development (T2). For control purposes, we performed similar analysis on counterpart organs from solvent-treated mice. Due to small size of lesions in mice at T1, the seminal vesicles of these animals were excluded from the analysis. Briefly, genomic DNA was isolated from either seminal vesicles or tumors developed at the same organ site and subjected to MIRA enrichment, as described previously (22). Following pull-down of the methylated CpG islands by MIRA, the enriched- and input DNA fractions were labeled, mixed and hybridized to the mouse CpG island plus promoter tiling arrays (Roche NimbleGen). The microarray data were normalized and analyzed using rigorous algorithms for peak calling, as described in ref. (22). Two independent lists of differentially methylated targets were generated based on the level of stringency used for data analysis, as follows: (i) stringent: methylation differences detected in four out of four biological replicates within a treatment group and absent in all respective controls and (ii) relaxed:

methylation differences detected in three out of four biological replicates within a treatment group and absent in all respective controls. When the stringent criteria were used for analysis, we identified 372 CpG targets that displayed aberrant methylation in tumors from B[a]P-treated animals relative to controls (251 hypermethylated and 121 hypomethylated CpG islands) (Figure 2A). A lower yet significant number of differentially methylated CpG islands was detected in the seminal vesicles of apparently asymptomatic mice treated with B[a]P at T0 (immediately after treatment), i.e. 123 aberrantly methylated targets, of which 60 were hypermethylated and 63 were hypomethylated (Figure 2A). Seventy-two percent of these 123 CpG islands coincide with those identified in tumors (T2), suggesting that aberrant DNA methylation in these targets occurs early in the process of tumorigenesis. Principal component analysis of the differentially methylated CpG islands confirmed that all samples within a treatment group clustered together, with a significant overlap between the T0 and T2 groups (Figure 2B and C). In tumors (T2), hypermethylated CpG islands map mostly within annotated genes (41%), whereas loss of methylation occurs predominantly at upstream regulatory regions (77%) (Figure 2D). Likewise, a characteristic pattern for genomic distribution of the aberrantly methylated targets was found in seminal vesicles of mice at T0, with 46% of hypermethylated CpG islands being intragenic and 76% of hypomethylated CpG islands mapping to the 5′-end of annotated genes (Figure 2D). The latter reaffirms that aberrant DNA methylation patterns are established immediately after carcinogen exposure, at a time preceding lesion formation (Figure 2D). We also observed that aberrant DNA methylation preferentially targets genes that are normally associated with either active histone mark (H3K4me3) or bivalent marks (H3K4me3 and H3K27me3) in murine embryonic stem cells (ESCs), as established by comparison of our data to published databases (30) (Figure 2E).

Validation of differentially methylated targets by COBRA and bisulfite sequencing

To validate the DNA methylation microarray results, we have randomly selected and analyzed several targets identified by MIRA-microarray analysis using the conventional COBRA (24) and bisulfite DNA sequencing (23). Representative COBRA results for hyper- and hypomethylated targets are shown in Figure 3A and B (upper panels) and Supplementary Figure S1, available at *Carcinogenesis* Online. In all cases, we confirmed DNA methylation differences between control and experimental samples collected at different time points posttreatment, which mirrored the differences observed in the array analysis. These confirmatory results indicate that epigenetic marks, i.e. CpG methylation, are established or lost during B[a]P-induced

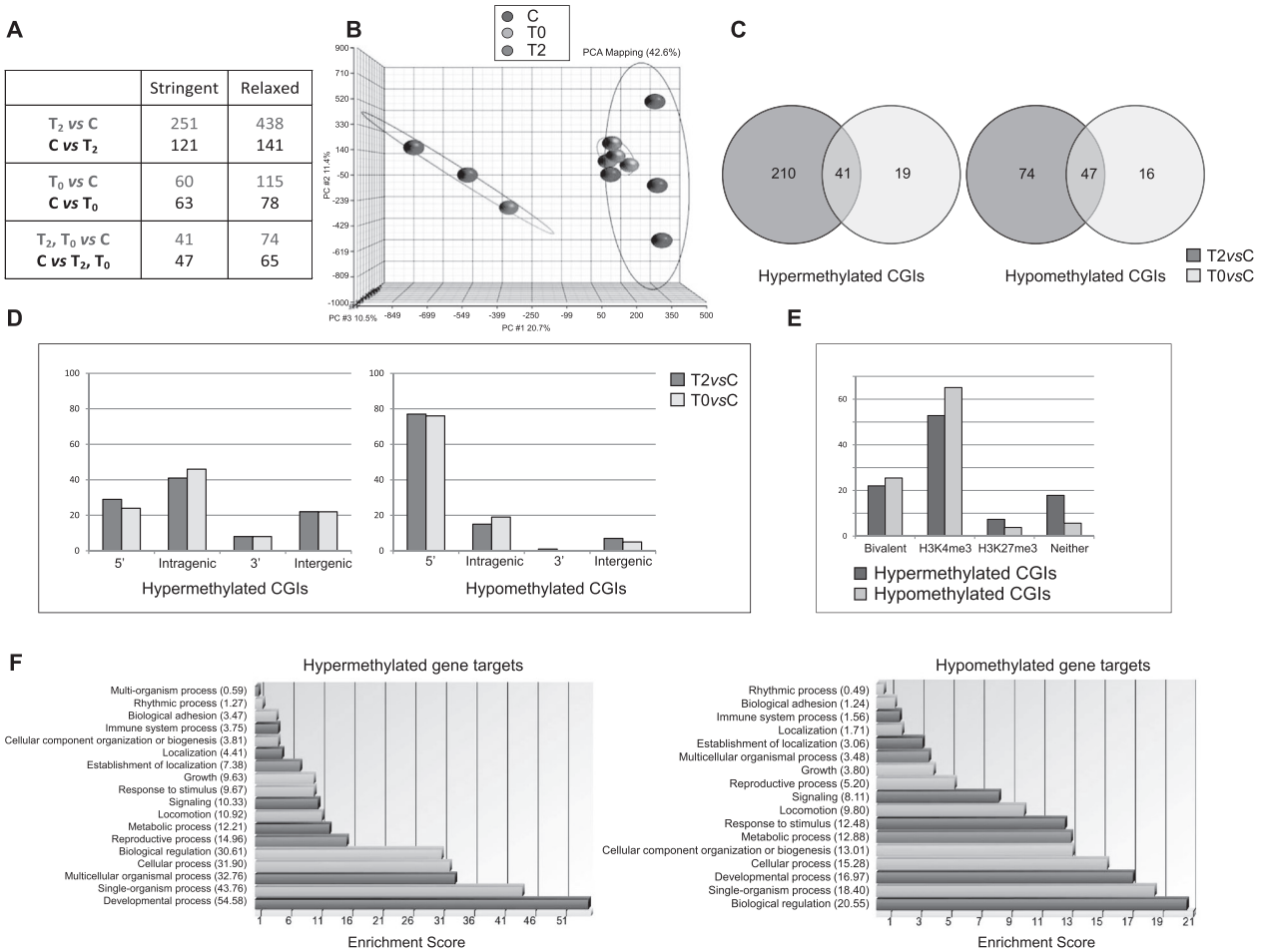

Fig. 2. Identification of differentially methylated targets in B[a]P-treated mice. (**A**) Aberrantly methylated CpG Islands were identified by MIRA-microarray analysis. Two independent lists of differentially methylated targets were generated based on the level of stringency used for data analysis, as described in the text. The minimum difference between groups was ≥2-fold. The numbers of methylation peaks within each dataset are shown (hypermethylated CpG Islands are in red). (**B**) Principal component analysis (PCA) of methylation data obtained in B[a]P-treated mice at T0 and T2 and control (C) using the Partek® software. (**C**) Venn diagrams of aberrantly methylated targets identified by MIRA-microarray analysis in B[a]P-treated mice at T0 (yellow) and T2 (blue) versus control. (**D**) Genomic localization of aberrantly methylated targets identified by MIRA-microarray analysis. (**E**) Colocalization of aberrantly methylated targets identified by MIRA-microarray analysis with histone marks established in ref. (30). (**F**) Gene ontology analysis by Partek® of relevant biological groups associated with hyper- and hypomethylated gene targets, respectively. Enrichment score: negative log of the enrichment *P* value. A high score indicates that the genes of a functional group are overrepresented in the gene list.

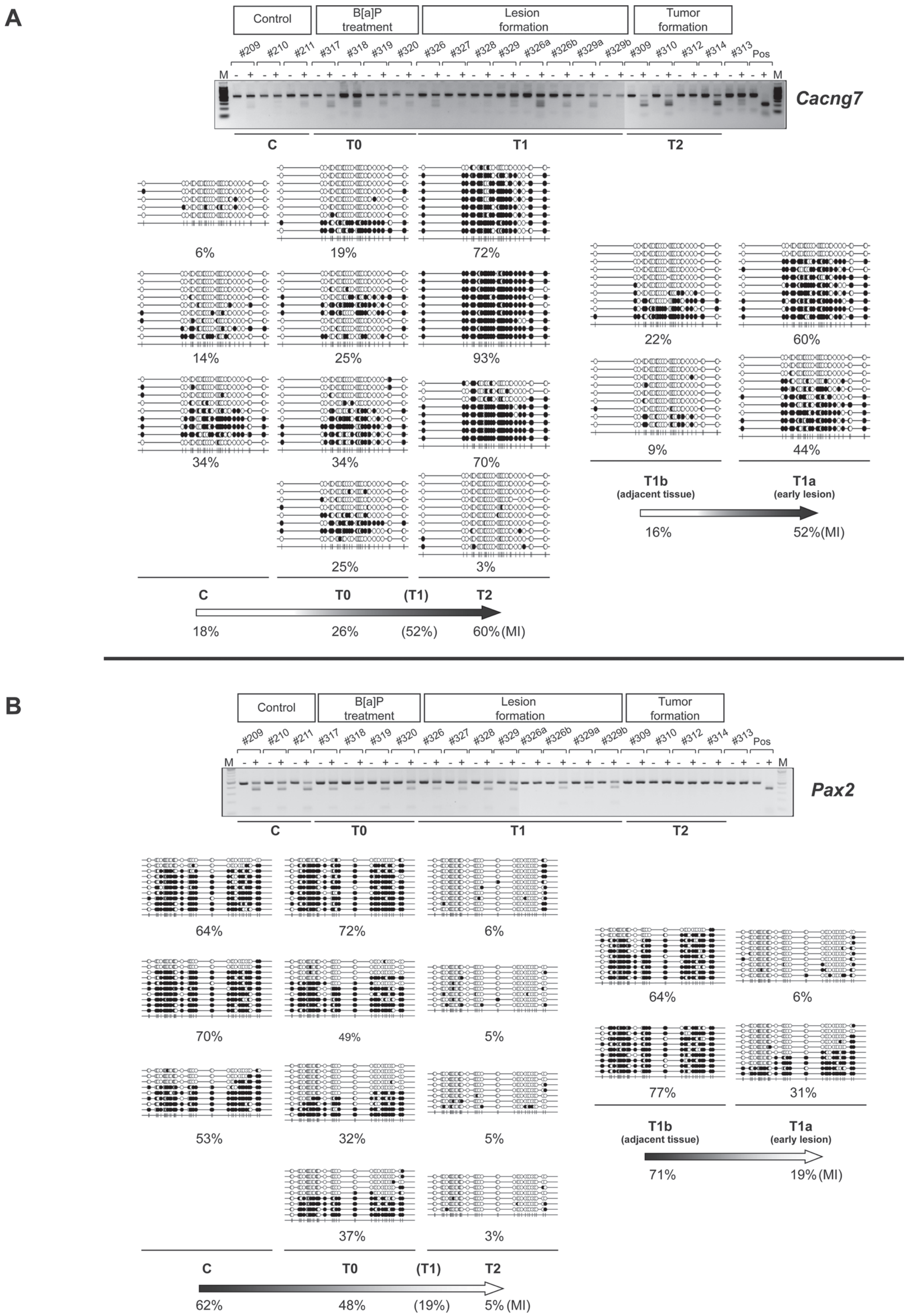

Fig. 3. Representative gene targets identified by MIRA-microarray analysis. (**A**) Top: genomic DNA from B[a]P-treated and control mice was treated with sodium bisulfite, and the hypermethylated CpG island downstream of the *Cacng7* gene was amplified with gene-specific primers and subjected to COBRA. Digested fragments on the gel are indicative of methylated restriction sites within the CpG island. *In vitro* methylated mouse genomic DNA served as positive control (Pos). The symbols (+) and (−) show the presence and absence, respectively, of the restriction enzyme in reaction mix. M = 100 bp ladder DNA marker. Bottom: the extent of CpG methylation in the *Cacng7*-associated CpG island was determined by sodium bisulfite sequencing in B[a]P-treated mice at T0 and T2 and control (C). The methylation status of precursor lesions (a) and adjacent normal tissues (b) in B[a]P-treated mice at T1 was also compared. The sequencing results of up to 10 independent clones and the respective percentage of methylation per sample are shown. Open and closed circles represent unmethylated and methylated CpG dinucleotides, respectively. MI = methylation index. (**B**) Top: COBRA analysis of the hypomethylated CpG island located downstream of the *Pax2* gene in B[a]P-treated mice. Digested fragments on the gel are indicative of methylated restriction sites within the CpG island. Bottom: the extent of CpG methylation within the *Pax2* CpG island was determined by sodium bisulfite sequencing in B[a]P-treated mice at T0 and T2 and control (C). The methylation status of precursor lesions (a) and adjacent normal tissues (b) in B[a]P-treated mice at T1 was also compared. The sequencing results of several independent clones and the respective percentage of methylation per sample are shown.

tumorigenesis. One of such targets is the *Cacng7* gene, whose product plays a role in the synaptic expression of cerebellar alpha-amino-3-hydroxy-5-methyl-4-isoxazolepropionic acid-type glutamate receptors (31). A normally unmethylated CpG island located downstream of the murine *Cacng7* gene becomes increasingly methylated immediately after treatment with B[a]P (T0), and thereafter (T1 and T2) (Figure 3A, top). A detailed methylation map for each CpG within the *Cacng7* CpG island was also constructed using the bisulfite sequencing technique (Figure 3A, bottom). A steady increase in the median percentage of CpG methylation at this locus was detectable in B[a]P-treated mice, as reflected in the methylation indices of 18, 26, 52 and 60% for samples of control, T0, T1 and T2 mice, respectively. Despite the substantial methylation increase in the *Cacng7* gene in precursor lesions of B[a]P-treated mice at T1, the methylation indices of this gene in the adjacent normal appearing tissues were comparable with that in solvent-treated controls. We have also verified B[a]P treatment-associated loss of methylation at several loci using both the COBRA and bisulfite sequencing. Figure 3B combines the COBRA and bisulfite sequencing results for a CpG island located 3′-end to the murine *Pax2*, a key gene involved in normal prostate development (32). DNA methylation at this downstream CpG island decreases immediately after the cessation of B[a]P treatment (from 62% in control animals to 48% in T0 mice to 19% in T1 mice) and is virtually lost in tumor-bearing animals at T2 (5%) (Figure 3B, bottom). Notwithstanding the loss of methylation in *Pax2* in early lesions of B[a]P-treated mice at T1, the surrounding apparently normal tissues had comparable methylation indices to that of DMSO-treated controls (Figure 3B, bottom). We have also detected agglomerate loss of methylation within gene families, e.g. the *Hoxa* and *Hoxb* homeobox gene clusters, a phenomenon commonly found in various types of human cancer (Supplementary Figure S2, available at *Carcinogenesis* Online) (33). Supplementary Table S2, available at *Carcinogenesis* Online, lists the hypermethylated and hypomethylated CpG islands identified in samples of mice at T0 and T2.

Methylation profiling of major repetitive DNA elements during B[a]P-induced tumorigenesis

To determine whether *in vivo* treatment of mice with B[a]P can induce global hypomethylation events, we have analyzed the methylation status of major repetitive DNA elements in the target organ of tumorigenesis in B[a]P-treated mice both before and after tumor development. Using a bisulfite sequencing-based approach (25), we determined the status of CpG methylation in LINE L1, IAP-LTR and SINE B1, which are routinely used as surrogate markers to estimate the overall DNA methylation level in the mouse genome (26–28). As shown in Supplementary Figure S3, available at *Carcinogenesis* Online, there was a significant reduction in CpG methylation in the IAP-LTR between experimental mice and controls ($P = 0.02$). However, no appreciable differences in CpG methylation were observed in the SINE B1 and LINE L1 between experimental and control mice.

Motif discovery

We next used the Partek® Genomics Suite™ Software (v 6.6) to search for common non-redundant sequence instances across the differentially methylated CpG islands in samples of B[a]P-treated mice at T0 and T2. The top-scored *de novo* motifs, identified by Partek analysis, are illustrated in Figure 4A and show an overall prevalence of purine residues (mostly guanines, followed by adenines), often in the context of CpG dinucleotides. Of note, B[a]P epoxy diols (B[a]PDE) are known to react with DNA to form covalent adducts preferentially at the *N2* position of guanines, and to a lesser extent, at *N6* position of adenines. It is well established that B[a]P-*N2*-dG adducts form more efficiently at methylated CpGs than non-methylated CpGs (18,19). We have also explored the occurrence of known transcription factor recognition sites within genomic loci targeted by aberrant DNA methylation during chemical carcinogenesis. A list of potential transcription factors with their respective consensus binding sites is shown in Figure 4B. Of interest, the non-histone *HMG-IY* transcription factor binds to A-T rich DNA sequences and participates in enhanceosome formation, chromatin remodeling and regulation of transcription, with a crucial role in many cellular processes, including cell growth and differentiation (34). Other potentially relevant transcription factors include the zinc finger protein *Mzf1*, which plays an important role in cell proliferation and tumorigenesis (35), and the forkhead box protein *Foxd3*, a novel epigenetically regulated tumor suppressor gene that controls ESC self-renewal and pluripotency as well as cell growth (Figure 4B) (36). Enrichment of consensus binding sites within the differentially methylated CpG islands indicates that aberrant DNA methylation can also interfere with *in vivo* binding of key transcription factors and/or recruitment of methyl-binding proteins (37).

Functional pathway analysis of differentially methylated genes

Using a combination of the Ingenuity Pathway Analysis® (IPA®: v 9.0) and the GO Enrichment Analysis in Partek® Genomics Suite™ (v 6.6), we obtained gene ontology information for the annotated genes identified as aberrantly methylated by MIRA-microarray analysis. Functional annotation analysis revealed that gene targets involved in connective tissue development and function, embryonic development, cell-to-cell signaling and interaction and nervous system development and function were particularly enriched (Figure 2F and IPA results). These target genes are members of the frequently disrupted signaling networks in cancer, including the *MEK/ERK*, *JAK/STAT3*, *PI3K/AKT*, *WNT/β-catenin* and *Shh* cascades (38–40) (Figure 5B and Supplementary Figure S4, available at *Carcinogenesis* Online). These signaling networks cross-talk to and modulate the *Nanog* pathway, which is overall the most represented canonical pathway, according to IPA (Figure 5A). The significance of the *Nanog* pathway in the establishment and maintenance of the pluripotent state and carcinogenesis is increasingly appreciated (see Discussion).

Correlation between DNA methylation and gene expression during B[a]P-induced carcinogenesis

To shed light into the underlying mechanisms of aberrant DNA methylation, we next measured the mRNA levels of major murine methyltransferases including the 'maintenance' *Dnmt1* and the '*de novo*' *Dnmt3a* and *Dnmt3b* methyltransferases. As shown in Figure 6A, we detected cumulative loss of expression of *Dnmt3a* and *Dnmt3b* in samples of B[a]P-treated mice both before (T0) and after tumor development (T2), whereas no significant changes were detectable in the expression level of *Dnmt1*. Misregulation of *Dnmt3a* and *Dnmt3b* can interfere with the establishment and maintenance of normal patterns of DNA methylation and, in turn, lead to tumorigenesis (41).

To investigate the impact of DNA methylation on gene expression during chemical carcinogenesis, we have also quantified the transcription level of several functionally important genes that were aberrantly methylated, as identified by our MIRA-microarray analysis. The examined genes are known components of the signaling cascades linked to the *Nanog* pathway and are potentially relevant for the establishment of a malignant phenotype (Figure 5B). Figure 6 shows the mean normalized expression levels of the *Wnt4* and *Fzd3* (Figure 6B), *Mapk3* (*Erk1*) and *Mapk11* (Figure 6C), *Foxd3*, *Nanog* and *Gata6* genes (Figure 6D) in samples of B[a]P-treated mice at T0 and T2 relative to control. With the exception of the *Gata6* gene, which is upregulated, most of the above genes show overall reduction in transcription levels during B[a]P-induced carcinogenesis.

Discussion

Chemical carcinogenesis has historically been accounted for by genotoxicity, which entails DNA damage, genetic mutations and chromosomal abnormalities (1–3). However, an emerging model of carcinogenicity recognizes that epigenetic alterations can also play an important role in the initiation and progression of cancer, although the underlying molecular mechanisms remain to be elucidated (4–6). To investigate whether epigenetic alterations are a determinant of

A

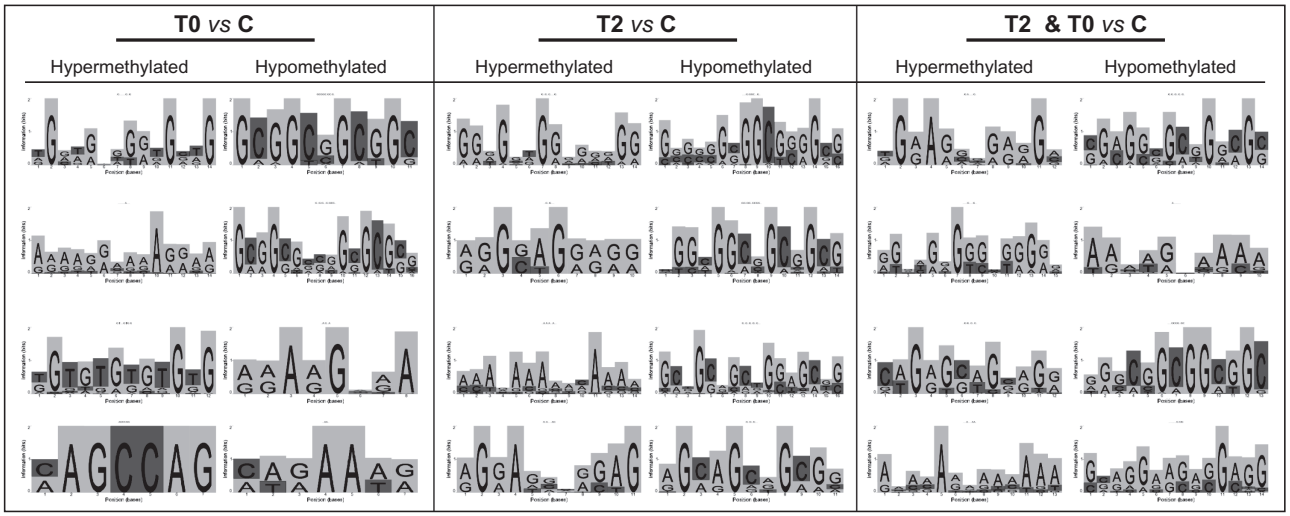

B

Motif	Consensus sequence	Probability of occurrence	Expected number of occurrences	Actual number of occurrences	p-value	
HMG-IY	CAACAAATGGAAAAAC	3.39E-06	0.260868	19	5.23E-29	T2 & T0 *vs* C Hypermethylated
hunchback (Pax1)	GCATAAAAAA	5.75E-05	4.42697	40	1.14E-24	
ID1	TTTTCCTTTTCG	5.37E-05	4.13683	37	8.48E-23	
Broad-complex_1	GTAATAAACAAATC	5.90E-06	0.454434	16	1.03E-19	
SPI1	CGGAAG	0.00193932	149.277	224	7.02E-09	
Broad-complex_4	TAGTAAACAAA	3.19E-05	2.45807	14	3.44E-07	
ABI4	CGGTGCCCCC	0.000538326	41.4371	76	9.45E-07	
MZF1_1-4	TGGGGA	0.00179311	138.023	192	7.98E-06	
Foxd3	GAATGTTTGTTT	1.00E-05	0.772267	7	1.66E-05	
MNB1A	AAAGC	0.00175662	135.214	186	1.99E-05	
HMG-IY	CAACAAATGGAAAAAC	2.72E-08	0.00167	27	9.44E-104	T2 & T0 *vs* C Hypomethylated
ID1	TTTTCCTTTTCG	1.97E-06	0.120647	41	5.77E-88	
hunchback (Pax1)	GCATAAAAAA	2.96E-06	0.181436	32	6.01E-60	
Broad-complex_1	GTAATAAACAAATC	8.65E-08	0.005309	18	1.74E-57	
Broad-complex_4	TAGTAAACAAA	1.73E-06	0.106152	24	6.07E-48	
Foxd3	GAATGTTTGTTT	3.45E-07	0.02116	14	4.05E-35	
Dof2	AAAGCA	0.000517022	31.7328	77	7.76E-12	
MNB1A	AAAGC	0.000480686	29.5026	71	6.88E-11	
PBF	AAAGC	0.000480686	29.5026	71	6.88E-11	
SQUA	CCAAAAATGGAAAT	1.16E-07	0.007118	3	5.98E-08	

Fig. 4. Summary of motif occurrences across differentially methylated CpG islands in B[a]P-treated mice at T0 and T2. (**A**) The top *de novo* motifs were selected using the Partek® Genomics Suite™ software and show high enrichment of guanines, often in the context of CpGs. The 'Sequence Logo' windows graphically display the best motifs found in the hyper- and hypomethylated CpG islands in samples of B[a]P-treated mice at T0 and T2. The height of each position is the relative entropy (in bits) and indicates the importance of a base at a particular location in the binding site. (**B**) Known motifs were identified by using the JASPAR database in Partek®, based on the number of occurrences above the threshold.

chemical carcinogenesis, we have chronicled changes in the epigenetic landscape during chemically induced carcinogenesis. Accordingly, we have assessed the alterations of the epigenome, as reflected in the patterns of DNA methylation, in mice treated *in vivo* with a representative chemical carcinogen, B[a]P (15), before and after tumor development. It is well established that rodents exposed to B[a]P develop large aggressive tumors (including sarcoma) at the accessory sex organs (29). Thus, we constructed the whole DNA methylome in the seminal vesicles or tumors formed at this organ site in B[a]P-treated mice at different intervals prior to (T0 and T1) and after tumor development (T2) (Figure 1A). Genome scale analysis, supported by standard validation assays, showed locus-specific hyper- and hypomethylation in B[a]P-treated mice, even at a time preceding detectable lesion formation. Of the 123 aberrantly methylated loci identified in the normal appearing seminal vesicles in B[a]P-treated mice at T0, a significant portion (72%) overlapped with those identified as tumor-specific differentially methylated targets in T2 mice (Figure 2A–C).

De novo motif discovery analysis of the aberrantly methylated CpG islands, in samples of B[a]P-treated mice at T0 and T2, indicates a high enrichment of guanine residues, often in the context of CpG dinucleotides (Figure 4A). This sequence specificity of the aberrantly methylated targets is consistent with preferential binding of the reactive metabolite of B[a]P, B[a]PDE, to guanines in the DNA (19). Given the fact that these epigenetic changes manifest early and in the absence of evident morphological abnormalities, it is tempting to speculate that these alterations are the initiating oncogenic events, directly related to the effect of carcinogen exposure, although a causal relationship remains to be established. At this time, we cannot exclude that other carcinogen-induced epigenetic effects, such as histone modifications, chromatin remodeling and/or microRNA gene modulation, may have triggered the aberration of DNA methylation patterns observed in the present study. Alternatively, it is plausible that the detected epigenetic changes are the result of B[a]P genotoxicity, e.g. mutations in crucial genes that can directly or indirectly influence key pathways involved in the establishment and maintenance of DNA methylation patterns. Of relevance, we observed downregulation of the '*de novo*' *Dnmt3a* and *Dnmt3b* methyltransferases (Figure 6A), which can lead to global loss of DNA methylation. In confirmation, we have found demethylation of the IAP-LTR repetitive elements in tumors of B[a]P-treated mice (Supplementary Figure S3, available at *Carcinogenesis* Online) (41). The IAP retrotransposons are often associated with 'metastable epialleles' in mouse, with varying methylation at specific CpG sites that can be influenced by *in utero* and/or early life exposure to environmental toxicants (6). Furthermore, we have detected agglomerates of differentially methylated CpG islands along extended chromosomal regions containing groups of consecutive genes, such as the *Hoxa* and *Hoxb* gene clusters, in B[a]P-treated mice both before

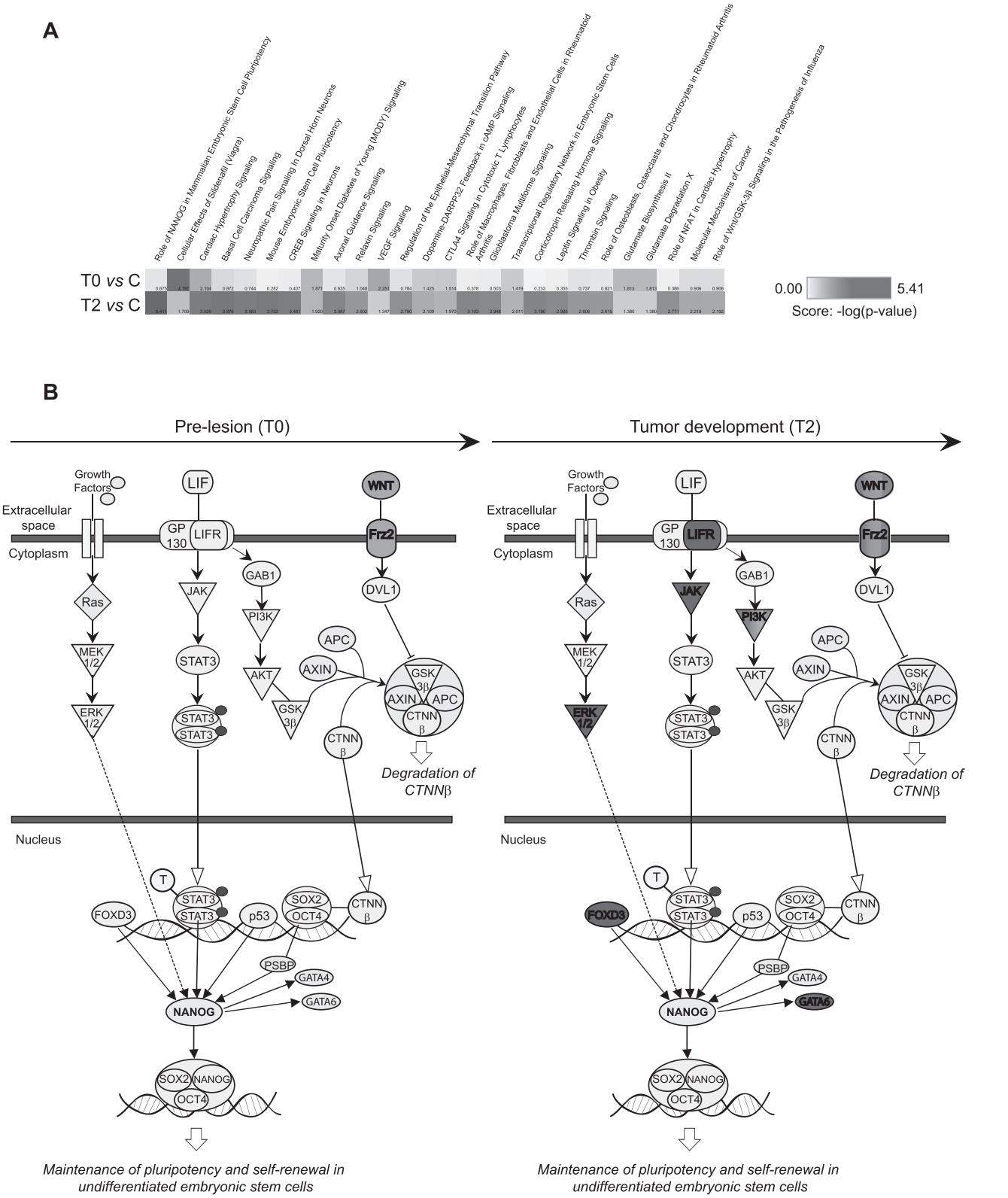

Fig. 5. Functional pathway analysis of aberrantly methylated genes in B[a]P-treated mice prior to (T0) and after (T2) tumor development. (**A**) The Canonical Pathway Heat Map was generated using the Comparison Analysis in IPA®. The heat map visualizes the enriched canonical pathways simultaneously in T0 and T2, allowing a direct comparison between the two datasets. The pathway scores are displayed using a blue color gradient, where darker blue corresponds to higher scores. The score represents the negative log of the *P* value derived from the Fisher's exact test. (**B**) The top canonical pathway (*Nanog* pathway) is crucial in mammalian ESC pluripotency and appears to play a role in chemical carcinogenesis. Aberrant DNA methylation targets several components of the signaling cascades that modulate *Nanog* expression and increases progressively from T0 to T2. Red and green nodes represent hyper- and hypomethylated gene targets identified by MIRA-microarray analysis, respectively. Adapted from IPA with some modifications.

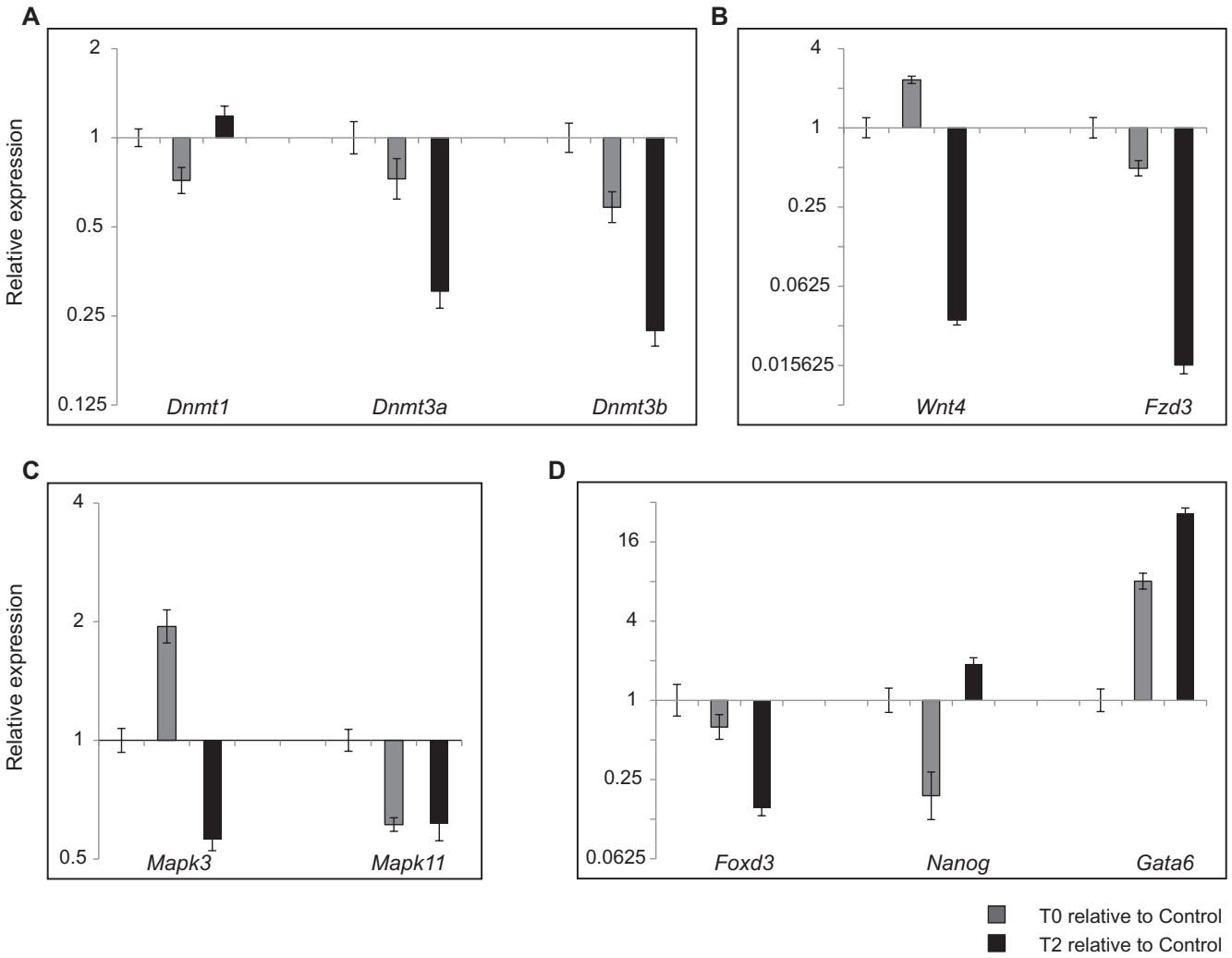

Fig. 6. Relative quantification of gene expression by standard qRT–PCR. The expression status of major methyltransferases and that of individual target genes identified by MIRA-microarray analysis was analyzed by standard qRT–PCR using the $2^{-\Delta\Delta C_t}$ method. Bars represent the mean normalized expression (±SD) of three replicates in samples of B[a]P-treated mice at T0 (gray) and T2 (black) relative to control. Data were normalized using an endogenous housekeeping gene as the reference (*Gapdh*) and untreated control as the calibrator (with expression equal to 1). Relative transcription levels of *Dnmt1*, *Dnmt3a* and *Dnmt3b* (**A**), *Wnt4* and *Fzd3* (**B**), *Mapk3* (*Erk1*) and *Mapk11* (**C**) and *Foxd3*, *Nanog* and *Gata6* genes (**D**) are shown.

and after tumor development (Supplementary Figure S2, available at *Carcinogenesis* Online). Agglomerative aberrant DNA methylation is an epigenetic signature commonly found in several types of human malignancy (33), cancer cell lines and other toxicant-induced models of cell transformation (42). Our overall data confirm that known hallmarks of human cancer, including locus-specific gain/loss of CpG methylation and global loss of methylation in repetitive DNA elements, are key components of chemically induced carcinogenesis.

In the present study, the identified tumor-specific aberrantly methylated genes colocalize mostly with the murine stem cell active histone marker (H3K4me3), and to a lesser extent, with the bivalent histone marker (H3K4me3 and H3K27me3), as deduced by comparing our methylation data with the published mouse databases (30) (Figure 2E). Nearly half of the annotated targets associated with the H3K4me3 active histone mark are phosphoproteins, mostly involved in intracellular signaling cascades. This is consistent with the functional pathway analysis that shows the convergence of top aberrantly methylated targets at the *MEK/ERK*, *JAK/STAT3, PI3K/AKT*, *WNT/β-catenin* and *Shh* signaling cascades. The annotated targets associated with bivalent marks are mainly involved in the control of transcription and pattern formation and include several developmental regulators. In agreement with findings by others (43,44), we have also found that 10% of the tumor-associated hypermethylated CpG islands overlap with loci that are bound by components of the polycomb repressive complex 1 (PRC1) (Rnf2 and Phc1) and PRC2 (Eed and Suz12) that are associated with transcriptionally silent chromatin in ESCs (45). Together, these data indicate an interplay between aberrant DNA methylation and histone modifications that shapes the epigenetic landscape during chemical carcinogenesis.

Gene ontology analysis of tumor-specific differentially methylated targets shows enrichment of genes involved in connective tissue development and function, embryonic development and organ development (Figure 2F and IPA results). The vast majority of these genes are normally expressed in the brain, a trend described in several human malignancies. The top canonical pathway whose members are preferential targets of aberrant DNA methylation is the *Nanog* pathway (Figure 5A). *Nanog* is a well-studied transcription factor that plays a crucial role in the maintenance and self-renewal of undifferentiated ESCs (46). *Nanog* expression is normally restricted to pluripotent cells and is downregulated upon differentiation; however, *Nanog* has also been found to be dysregulated in cancer cell lines and tumors (47). Accumulating evidence supports that *Nanog* and other pluripotency genes can function as neoplastic engines to drive tumorigenesis, probably promoting infinite self-renewal of a distinct subset of stem-like cells within tumors (46,48). Interestingly, we have observed methylation defects in genes upstream of *Nanog*, particularly in

components of the oncogenic signaling cascades, including the *MEK/ERK*, *JAK/STAT3*, and *WNT/β-catenin*, etc., which modulate *Nanog* expression.

Consistent with DNA methylation data, standard qRT–PCR analysis confirmed abnormal and deregulated expression of several components of the signaling cascades interconnected with the *Nanog* pathway, which may altogether cause perturbations in cell fate decision and differentiation and, ultimately, lead to cancer (Figure 6B–D). Apart from altering the expression of key genes (i.e. transcription factors), aberrant DNA methylation can also disrupt their respective genomic binding sites, thus, interfering with regulation of downstream effectors. For instance, epigenetic downregulation of the *Foxd3* gene (Supplementary Table S2, available at *Carcinogenesis* Online and Figure 6D) and functional inactivation of *Foxd3* recognition sites by aberrant DNA methylation (Figure 4B) can both contribute to loss of *Foxd3* tumor suppressive function. Of note, ~10% of the cancer-related hypermethylated genes identified in this study are potential binding targets of *Nanog* in murine ESCs (49). Our findings accord with a recent report by Varley *et al.* (50) who demonstrated that cancer-specific hypermethylation is enriched at sites bound by *Nanog* in human ESCs.

In summary, our study indicates that *in vivo* exposure of mice to a prototype chemical carcinogen can alter the epigenetic landscape in a similar fashion to that found in human cancer. The alterations of the epigenome, as reflected in the patterns of DNA methylation, progressively increase during chemical carcinogenesis. Members of the *Nanog* pathway, which establishes and maintains pluripotency in the mammalian ESCs and possibly triggers uncontrolled proliferation of neoplastic cells (46), are preferential targets of aberrant DNA methylation during chemical carcinogenesis. Moreover, top gene networks targeted by aberrant DNA methylation are components of the signaling cascades that cross-talk to *Nanog* and are frequently disrupted in human cancer. Altogether, our data show the predictive value of aberrant DNA methylation in carcinogenesis and the potential utility of this epigenetic mark for early detection and monitoring of the progression of malignancy. Given the reversibility of this epigenetic change, e.g. through pharmacologic interventions, mitigating aberrant DNA methylation, particularly at the loci and in the pathways identified in the present study, may serve as a therapeutic approach for cancer.

Supplementary material

Supplementary Tables S1 and S2 and Figures S1–S4 can be found at http://carcin.oxfordjournals.org/

Funding

American Cancer Society (RSG-11-083-01-CNE); University of California Tobacco Related Disease Research Program (20XT-0116 to A.B.).

Acknowledgements

We thank Meng Li, from the NML Bioinformatics Service Program of the University of Southern California, for help with the Partek® Genomics Suite™ software. We also thank the City of Hope Bioinformatics Core Facility for initial microarray data analysis and Dr Sharon Wilczynski, from the Department of Anatomic Pathology, for help with H&E analysis.

Conflict of Interest Statement: None declared.

References

1. Luch,A. (2005) Nature and nurture - lessons from chemical carcinogenesis. *Nat. Rev. Cancer*, **5**, 113–125.
2. Loeb,L.A. *et al.* (2008) Advances in chemical carcinogenesis: a historical review and prospective. *Cancer Res.*, **68**, 6863–6872.
3. Wogan,G.N. *et al.* (2004) Environmental and chemical carcinogenesis. *Semin. Cancer Biol.*, **14**, 473–486.
4. Cortessis,V.K. *et al.* (2012) Environmental epigenetics: prospects for studying epigenetic mediation of exposure-response relationships. *Hum. Genet.*, **131**, 1565–1589.
5. Pogribny,I.P. *et al.* (2013) Environmental toxicants, epigenetics, and cancer. *Adv. Exp. Med. Biol.*, **754**, 215–232.
6. Bollati,V. *et al.* (2010) Environmental epigenetics. *Heredity (Edinb).*, **105**, 105–112.
7. Portela,A. *et al.* (2010) Epigenetic modifications and human disease. *Nat. Biotechnol.*, **28**, 1057–1068.
8. Baylin,S.B. *et al.* (2011) A decade of exploring the cancer epigenome - biological and translational implications. *Nat. Rev. Cancer*, **11**, 726–734.
9. Jones,P.A. (2012) Functions of DNA methylation: islands, start sites, gene bodies and beyond. *Nat. Rev. Genet.*, **13**, 484–492.
10. Deaton,A.M. *et al.* (2011) CpG islands and the regulation of transcription. *Genes Dev.*, **25**, 1010–1022.
11. Maunakea,A.K. *et al.* (2010) Conserved role of intragenic DNA methylation in regulating alternative promoters. *Nature*, **466**, 253–257.
12. Ehrlich,M. (2009) DNA hypomethylation in cancer cells. *Epigenomics*, **1**, 239–259.
13. Nagarajan,R.P. *et al.* (2009) Epigenetic mechanisms in glioblastoma multiforme. *Semin. Cancer Biol.*, **19**, 188–197.
14. Wilson,A.S. *et al.* (2007) DNA hypomethylation and human diseases. *Biochim. Biophys. Acta*, **1775**, 138–162.
15. Besaratinia,A. *et al.* (2005) DNA damage and mutagenesis induced by polycyclic aromatic hydrocarbons. In Luch,A. (ed.) *The Carcinogenic Effects of Polycyclic Aromatic Hydrocarbons*. Imperial College Press, London, UK, pp. 171–210.
16. Weisenberger,D.J. *et al.* (1999) Cytosine methylation in a CpG sequence leads to enhanced reactivity with Benzo[a]pyrene diol epoxide that correlates with a conformational change. *J. Biol. Chem.*, **274**, 23948–23955.
17. Wojciechowski,M.F. *et al.* (1984) Inhibition of DNA methyltransferases *in vitro* by benzo[a]pyrene diol epoxide-modified substrates. *J. Biol. Chem.*, **259**, 9711–9716.
18. Wilson,V.L. *et al.* (1983) Inhibition of DNA methylation by chemical carcinogens *in vitro*. *Cell*, **32**, 239–246.
19. Stone,M.P. *et al.* (2011) Chemistry and structural biology of DNA damage and biological consequences. *Chem. Biodivers.*, **8**, 1571–1615.
20. Huidobro,C. *et al.* (2013) The role of genetics in the establishment and maintenance of the epigenome. *Cell. Mol. Life Sci.*, **70**, 1543–1573.
21. Dolinoy,D.C. *et al.* (2008) Environmental epigenomics in human health and disease. *Environ. Mol. Mutagen.*, **49**, 4–8.
22. Tommasi,S. *et al.* (2013) Mammalian cells acquire epigenetic hallmarks of human cancer during immortalization. *Nucleic Acids Res.*, **41**, 182–195.
23. Frommer,M. *et al.* (1992) A genomic sequencing protocol that yields a positive display of 5-methylcytosine residues in individual DNA strands. *Proc. Natl Acad. Sci. USA*, **89**, 1827–1831.
24. Xiong,Z. *et al.* (1997) COBRA: a sensitive and quantitative DNA methylation assay. *Nucleic Acids Res.*, **25**, 2532–2534.
25. Yang,A.S. *et al.* (2004) A simple method for estimating global DNA methylation using bisulfite PCR of repetitive DNA elements. *Nucleic Acids Res.*, **32**, e38.
26. Goodier,J.L. *et al.* (2001) A novel active L1 retrotransposon subfamily in the mouse. *Genome Res.*, **11**, 1677–1685.
27. Martens,J.H. *et al.* (2005) The profile of repeat-associated histone lysine methylation states in the mouse epigenome. *EMBO J.*, **24**, 800–812.
28. Waterston,R.H., *et al.* (2002) Initial sequencing and comparative analysis of the mouse genome. *Nature*, **420**, 520–562.
29. Moore,R.A., *et al.* (1937) Production of tumors of the prostate of the white rat with 1:2-benzpyrene. *Am J Cancer.*, **30**, 731–741.
30. Rugg-Gunn,P.J. *et al.* (2010) Distinct histone modifications in stem cell lines and tissue lineages from the early mouse embryo. *Proc. Natl Acad. Sci. USA*, **107**, 10783–10790.
31. Yamazaki,M. *et al.* (2010) TARPs gamma-2 and gamma-7 are essential for AMPA receptor expression in the cerebellum. *Eur. J. Neurosci.*, **31**, 2204–2220.
32. Xu,B. *et al.* (2012) The role of Pax2 in mouse prostate development. *Prostate*, **72**, 217–224.
33. Ordway,J.M. *et al.* (2006) Comprehensive DNA methylation profiling in a human cancer genome identifies novel epigenetic targets. *Carcinogenesis*, **27**, 2409–2423.
34. Massimi,I. *et al.* (2013) The HMGA1 protoncogene frequently deregulated in cancer is a transcriptional target of E2F1. *Mol. Carcinog.*, **52**, 526–534.
35. Gaboli,M. *et al.* (2001) Mzf1 controls cell proliferation and tumorigenesis. *Genes Dev.*, **15**, 1625–1630.

36. Liu,Y. *et al.* (2008) Regulation of embryonic stem cell self-renewal and pluripotency by Foxd3. *Stem Cells*, **26**, 2475–2484.
37. Suzuki,M.M. *et al.* (2008) DNA methylation landscapes: provocative insights from epigenomics. *Nat. Rev. Genet*., **9**, 465–476.
38. Schubbert,S. *et al.* (2007) Hyperactive Ras in developmental disorders and cancer. *Nat. Rev. Cancer*, **7**, 295–308.
39. Carnero,A. (2010) The PKB/AKT pathway in cancer. *Curr. Pharm. Des*., **16**, 34–44.
40. Katoh,Y. *et al.* (2009) Hedgehog target genes: mechanisms of carcinogenesis induced by aberrant hedgehog signaling activation. *Curr. Mol. Med*., **9**, 873–886.
41. Jurkowska,R.Z. *et al.* (2011) Structure and function of mammalian DNA methyltransferases. *Chembiochem*, **12**, 206–222.
42. Severson,P.L. *et al.* (2012) Agglomerates of aberrant DNA methylation are associated with toxicant-induced malignant transformation. *Epigenetics*, **7**, 1238–1248.
43. Widschwendter,M. *et al.* (2007) Epigenetic stem cell signature in cancer. *Nat. Genet*., **39**, 157–158.
44. Fernandez,A.F. *et al.* (2012) A DNA methylation fingerprint of 1628 human samples. *Genome Res*., **22**, 407–419.
45. Boyer,L.A. *et al.* (2006) Polycomb complexes repress developmental regulators in murine embryonic stem cells. *Nature*, **441**, 349–353.
46. Saunders,A. *et al.* (2013) Concise review: pursuing self-renewal and pluripotency with the stem cell factor Nanog. *Stem Cells*, **31**, 1227–1236.
47. Wang,M.L. *et al.* (2013) Targeting cancer stem cells: emerging role of Nanog transcription factor. *Onco. Targets. Ther*., **6**, 1207–1220.
48. Luo,Y., *et al.* (2012) Cell signalling regulates dynamics of Nanog distribution in embryonic stem cell populations. *J R Soc Interface*., [epub ahead of print].
49. Loh,Y.H. *et al.* (2006) The Oct4 and Nanog transcription network regulates pluripotency in mouse embryonic stem cells. *Nat. Genet*., **38**, 431–440.
50. Varley,K.E. *et al.* (2013) Dynamic DNA methylation across diverse human cell lines and tissues. *Genome Res*., **23**, 555–567.

Received September 10, 2013; revised January 8, 2014; accepted January 17, 2014

FIGURE LEGENDS

Figure S1. Verification of differentially methylated CpG islands by COBRA. Genomic DNA from B[a]P-treated and control mice was treated with sodium bisulfite, and the CpG islands of interest were amplified with gene-specific primers, and subjected to COBRA. Digested fragments on the gel are indicative of methylated restriction sites within the CpG island. *In vitro* methylated mouse genomic DNA served as positive control (Pos). The symbols (+) and (-) show the presence and absence, respectively, of the restriction enzyme in the reaction mix. M= 100 bp ladder DNA marker.

Figure S2. Hypermethylated CpG islands associated with the *Hoxa* and *Hoxb* clusters. Visualization of the NimbleGen array data for B[a]P-treated (T0, in blue and T2, in red) and control mice (C, in green). At this level of resolution, each peak corresponds to a CpG island. The methylation signal, obtained by the NimbleScan software, is plotted along the chromosome as a *P*-value on the *y*-axis (starting from 0 when *P*-value is 1). The *P*-value is derived from the Kolmogorov–Smirnov test comparing the log2 enrichment ratios between MIRA and input within a 750 bp window.

Figure S3. Methylation profiling in repetitive DNA elements in tumors from B[a]P-treated mice. (**A**) Bisulfite sequencing of LINE L1, IAP-LTR and SINE B1 elements. Values indicate percentages of mCpGs. (**B**) Quantification of mCpGs in major repetitive DNA elements in tumors from B[a]P-treated mice *versus* control. Fisher's exact test was used to calculate the statistical significance of difference in mCpGs between tumors and controls.

Figure S4. Functional pathway analysis of aberrantly methylated genes in tumors from B[a]P-treated mice. Merging networks were generated by Ingenuity Pathway Analysis® (IPA®: v 9.0), using the relaxed list (T2 *vs* C). The convergence of genes in the *MEK/ERK*, *AKT* and *Shh* networks is noticeable. Red and green nodes represent hypermethylated and hypomethylated genes, respectively.

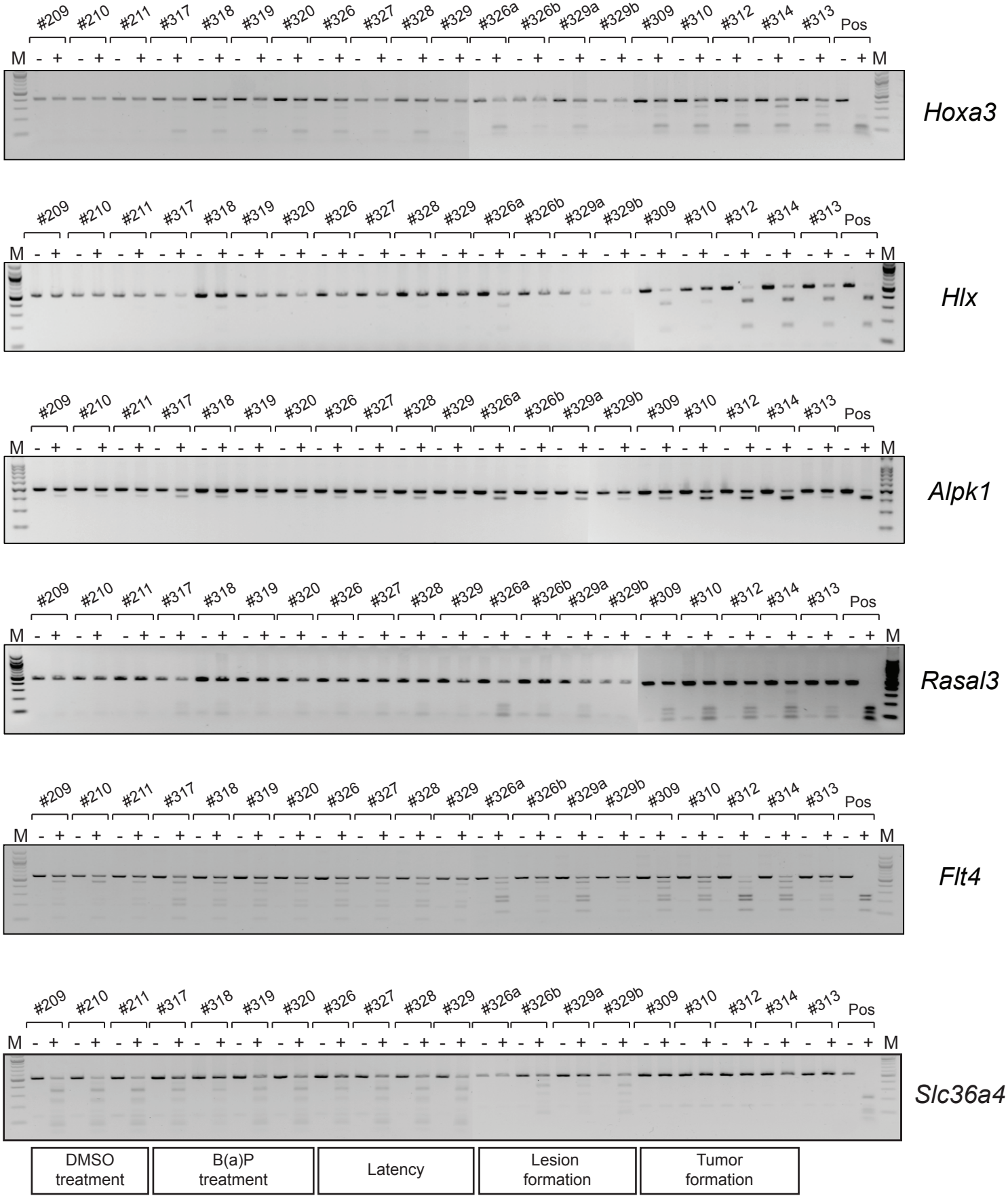
#209 #210 #211 #317 #318 #319 #320 #326 #327 #328 #329 #326a #326b #329a #329b #309 #310 #312 #314 #313 Pos
M
Hoxa3
Hlx
Alpk1
Rasal3
Flt4
Slc36a4
DMSO treatment
B(a)P treatment
Latency
Lesion formation
Tumor formation

Figure S1

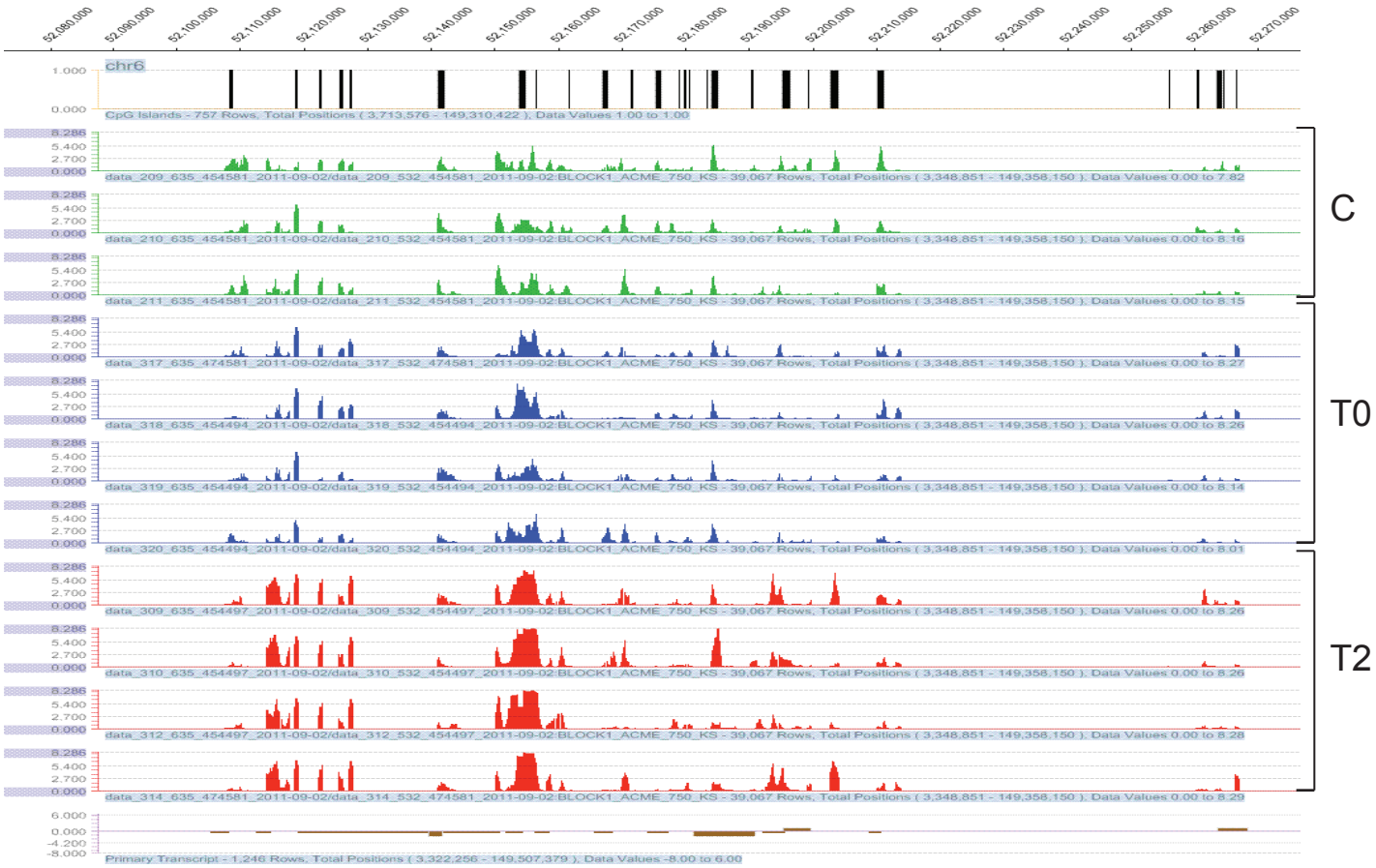

Hoxa cluster

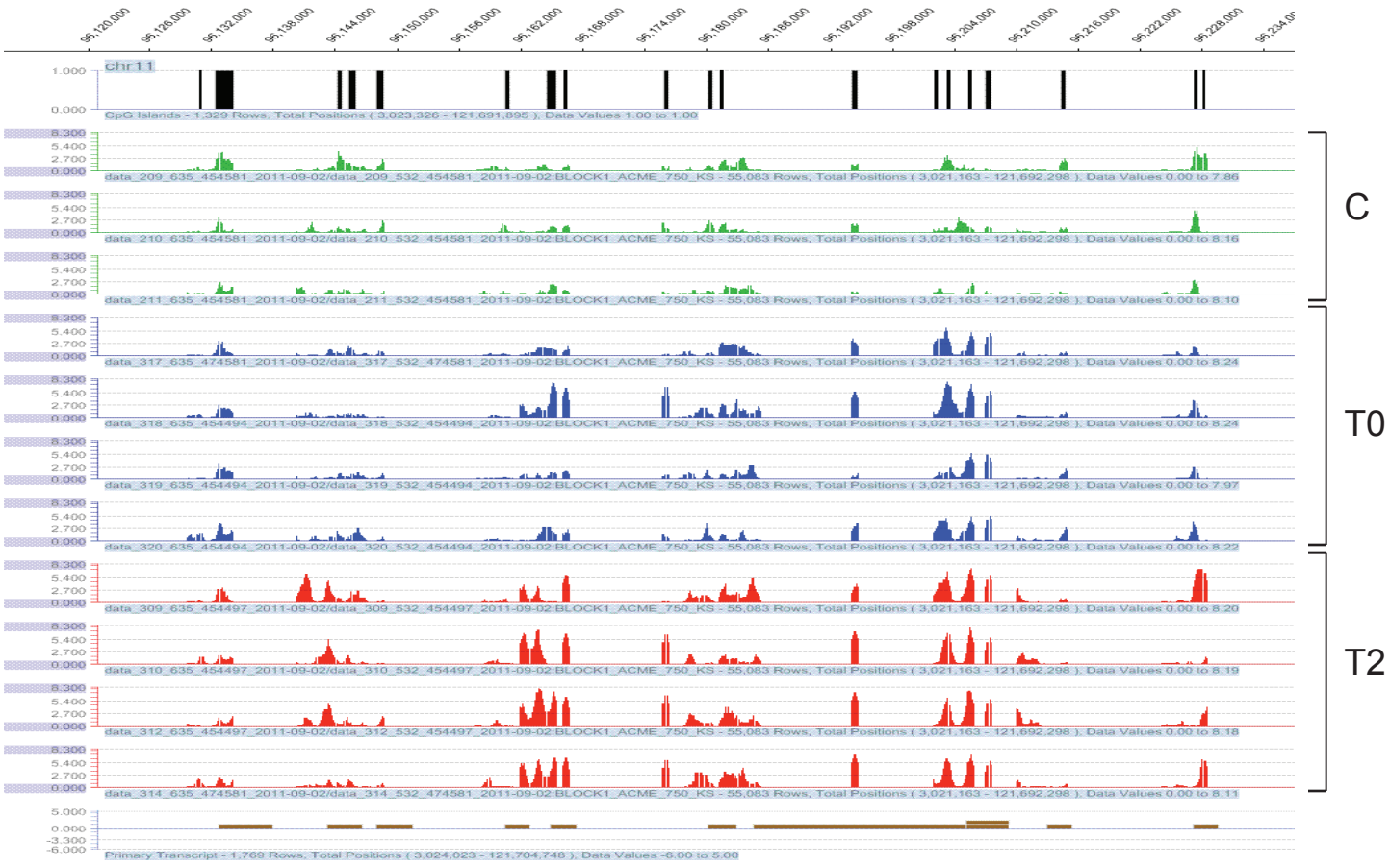

Hoxb cluster

Figure S2

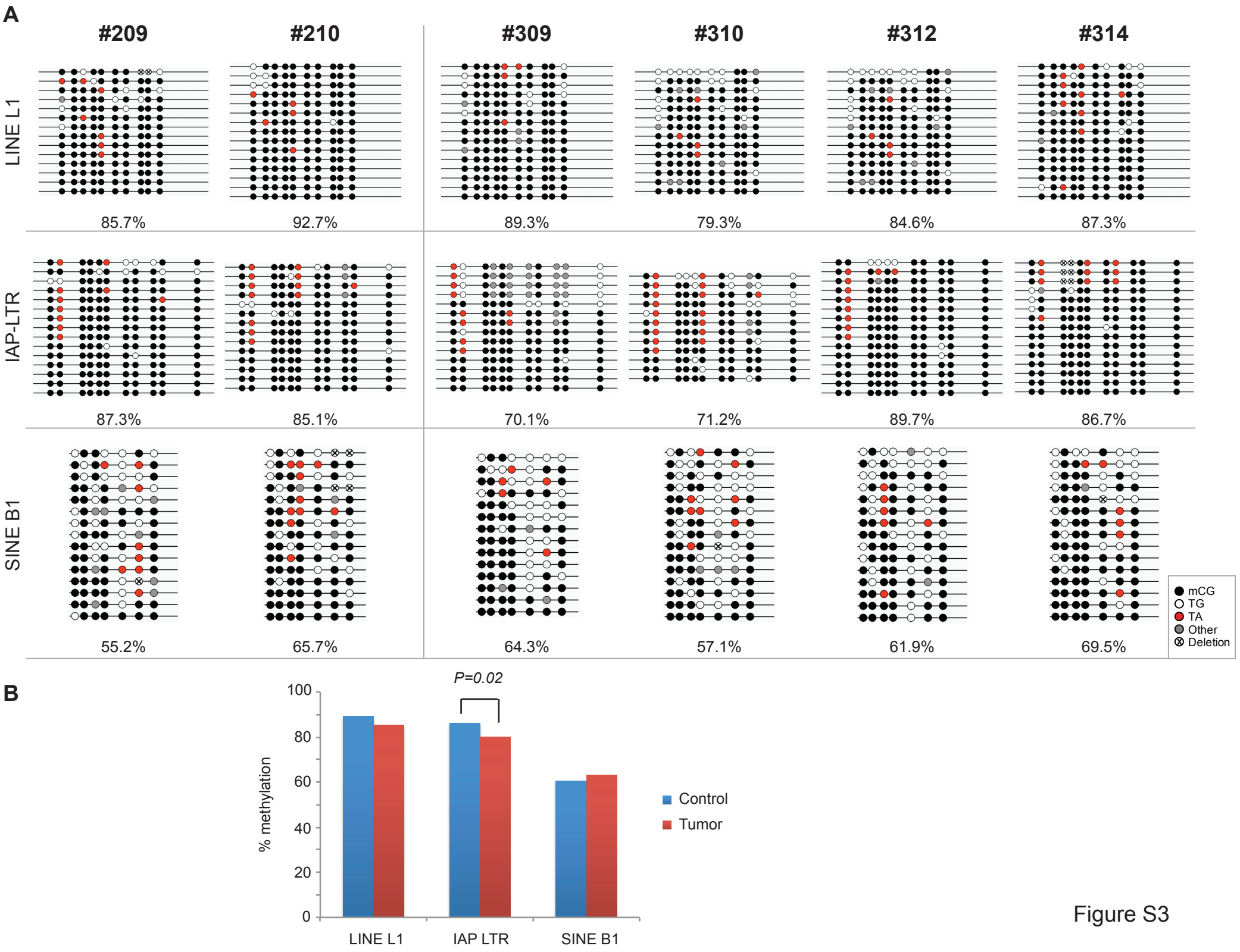
A
#209
#210
#309
#310
#312
#314
LINE L1
85.7%
92.7%
89.3%
79.3%
84.6%
87.3%
IAP-LTR
87.3%
85.1%
70.1%
71.2%
89.7%
86.7%
SINE B1
55.2%
65.7%
64.3%
57.1%
61.9%
69.5%
mCG
TG
TA
Other
Deletion
B
P=0.02
100
80
60
40
20
0
% methylation
LINE L1
IAP LTR
SINE B1
Control
Tumor

Figure S3

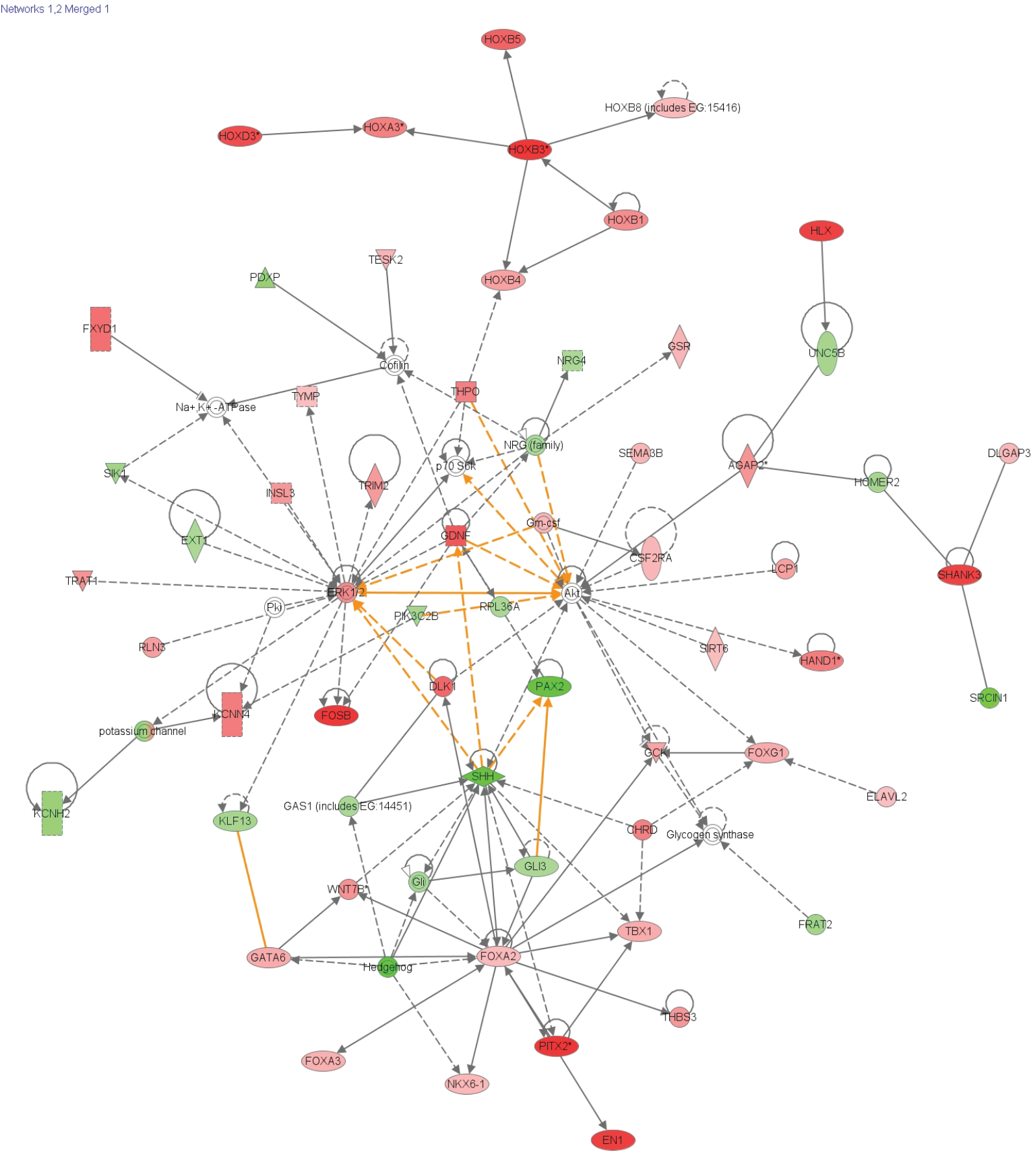
Networks 1,2 Merged 1
HOXB5
HOXB8 (includes EG:15416)
HOXD3*
HOXA3*
HOXB3*
HOXB1
HLX
TESK2
PDXP
HOXB4
FXYD1
Cofilin
NRG4
GSR
UNC5B
Na+,K+-ATPase
TYMP
THPO
NRG (family)
SEMA3B
AGAP2*
DLGAP3
SIK1
p70 S6k
HOMER2
INSL3
TRIM2
EXT1
Gm-csf
GDNF
CSF2RA
LCP1
SHANK3
TRAF1
ERK1/2
Akt
Pkj
PIK3C2B
RPL36A
RLN3
SIRT6
HAND1*
DLK1
PAX2
SRCIN1
FOSB
KCNN4
potassium channel
GCH
FOXG1
SHH
KCNH2
KLF13
GAS1 (includes EG:14451)
ELAVL2
CHRD
Glycogen synthase
GLI3
Gli
WNT7B*
FRAT2
TBX1
GATA6
FOXA2
Hedgehog
THBS3
PITX2*
FOXA3
NKX6-1
EN1

Figure S4

Table S1. Primers used for qRT-PCR

Gene symbol	Forward	Reverse	Product size (bp)
Gata6	5'-TTGCTCCGGTAACAGCAGTG	5'-GTGGTCGCTTGTGTAGAAGGA	105
Mapk11	5'-TCAGTGCGGCCGAAGCCTTG	5'-CGTGCGCTCCTTGGCCTCAA	110
Wnt4	5'-AGACGTGCGAGAAACTCAAAG	5'-GGAACTGGTATTGGCACTCCT	126
Mapk3	5'-TCCGCCATGAGAATGTTATAGGC	5'-GGTGGTGTTGATAAGCAGATTGG	248
Fzd3	5'-ATGGCTGTGAGCTGGATTGTC	5'-GGCACATCCTCAAGGTTATAGGT	109
Nanog	5'-TCTTCCTGGTCCCCACAGTTT	5'-GCAAGAATAGTTCTCGGGATGAA	100
Foxd3	5'-GACCCCGAACAAGCCCAAG	5'-GAAAACGGTTGCTGATGAACTC	137
Dnmt1	5'-CCTAGTTCCGTGGCTACGAGGAGAA	5'-TCTCTCTCCTCTGCAGCCGACTCA	137
Dnmt3a	5'-GCCGAATTGTGTCTTGGTGGATGACA	5'-CCTGGTGGAATGCACTGCAGAAGGA	147
Dnmt3b	5'-TTCAGTGACCAGTCCTCAGACACGAA	5'-TCAGAAGGCTGGAGACCTCCCTCTT	145
Gapdh	5'-AGGTCGGTGTGAACGGATTTG	5'-TGTAGACCATGTAGTTGAGGTCA	123

Table S2. List of differentially methylated CGIs in B[a]P-treated mice *versus* control

Hypermethylated CGIs

T2 vs C

	chr	start	end	NCaseV	NContrc	caseVScontrol	prc	promoter.Star	promoter.End	promoter.Sym	promoter.Acc	intr	intragenic.Star	intragenic.End	intragenic.Sym	intragenic.Acc	dov	downstream.S	downstream.E	downstream.S	downstream.Accession
1	chr3	128921352	128922021	4	3	3.8											+	128921508	128923508	Pitx2	NM_011098
2	chr11	96207041	96207580	4	3	3.75						+	96206082	96208244	Hoxb3	NM_010458					
3	chr7	19890073	19890732	4	3	3.71						-	19889044	19894394	Fosb	NM_008036					
4	chr1	186551383	186552042	4	3	3.49											-	186550023	186552023	Hlx	NM_008250
5	chr15	89378099	89378958	4	3	3.47						+	89331287	89389691	Shank3	NM_021423					
6	chr2	74570599	74571243	4	3	3.23						+	74551049	74585328	Hoxd3	NM_010468					
7	chr11	49447365	49447999	4	3	3.17						+	49424180	49465241	Flt4	NM_008029					
8	chr3	128918504	128919173	4	3	3.13						+	128903841	128921508	Pitx2	NM_001042504					
9	chr11	96205079	96205930	4	3	3.05	+	96204082	96206082	Hoxb3	NM_010458	+	96185439	96208244	Hoxb3	NM_001079869					
10	chr15	103000379	103000923	4	3	3.05															
11	chr6	125031667	125032316	4	3	2.98											+	125031490	125033490	Lpar5	NM_001163268
12	chr11	85654095	85654768	4	3	2.9						+	85647116	85654450	Tbx2	NM_009324					
13	chr3	96488547	96489208	4	3	2.9						+	96475053	96493957	Ankrd35	NM_001081139					
14	chr11	96166037	96166716	4	3	2.79						+	96165825	96166435	Hoxb5	NM_008268					
15	chr2	130997009	130997678	4	3	2.79						-	130996996	130999546	Spef1	NM_027641					
16	chr3	127398178	127398802	4	3	2.76						-	127374227	127482445	Alpk1	NM_027808					
17	chr8	73121934	73122603	4	3	2.76											-	73120388	73122388	Ssbp4	NM_133772
18	chr12	110697768	110698417	4	3	2.73						+	110692664	110700546	Dlk1	NM_001190703					
19	chr11	85650325	85650774	4	3	2.71						+	85647116	85654450	Tbx2	NM_009324					
20	chr5	135752281	135752928	4	3	2.71															
21	chr12	81210829	81211463	4	3	2.67						-	81209746	81213000	Zfp36l1	NM_007564					
22	chr2	9796091	9796760	4	3	2.63						-	9779704	9799227	Gata3	NM_008091					
23	chr14	22804205	22804839	4	3	2.62						-	22804183	22807823	Zfp503	NM_145459					
24	chr7	20204681	20205230	4	3	2.6						-	20192570	20213787	Relb	NM_009046					
25	chr6	48487311	48487880	4	3	2.56	+	48486567	48488567	Atp6v0e2	NM_133764										
26	chr11	98797343	98797977	4	3	2.55															
27	chr2	74584434	74585386	4	3	2.55						+	74551049	74585328	Hoxd3	NM_010468					
28	chr10	126763394	126764345	4	3	2.51						+	126761782	126765999	Arhgap9	NM_146011					
29	chr7	148650604	148650973	4	3	2.51						+	148647992	148651501	Efcab4a	NM_001025103					
30	chr8	90186286	90186843	4	3	2.48											-	90184708	90186708	Zfp423	NM_033327
31	chrX	35533991	35534520	4	3	2.47															
32	chr13	55515975	55516823	4	3	2.46	-	55515593	55517593	Pfn3	NM_029303	-	55516048	55516593	Pfn3	NM_029303	-	55515048	55517048	Pfn3	NM_029303
33	chr16	94083599	94084043	4	3	2.45															
34	chr16	20734247	20734991	4	3	2.43	-	20733584	20735584	Thpo	NM_009379	+	20734199	20741457	Chrd	NM_009893					
35	chr2	25433799	25434748	4	3	2.43						-	25431935	25434619	Gm996	NM_001005424					
36	chr7	108445030	108445694	4	3	2.41						-	108439129	108449602	Atg16l2	NM_001111111					
37	chr16	17804184	17804813	4	3	2.4						+	17798374	17807380	Scarf2	NM_153790					
38	chr8	90183994	90184633	4	3	2.39															
39	chr3	88339915	88340974	4	3	2.38	-	88339304	88341304	Mir1905	NR_035434	+	88337316	88344316	Mex3a	NM_0010298	-	88339222	88341222	Mir1905	NR_035434
40	chr17	56095347	56095976	4	3	2.37											+	56095445	56097445	Ebi3	NM_015766
41	chr9	21116345	21117189	4	3	2.37	-	21115777	21117777	Ap1m2	NM_001110300										
42	chr16	88562691	88563140	4	3	2.35	-	88562428	88564428	Cldn8	NM_018778										
43	chr5	120132506	120133157	4	3	2.35						+	120121677	120133610	Tbx3	NM_198052					
44	chr5	113566789	113567258	4	3	2.34						-	113516342	113591333	2900026A02Ri	NM_172884					
45	chr11	57642726	57643407	4	3	2.33											-	57641214	57643214	Hand1	NM_008213
46	chr4	151493444	151494103	4	3	2.33											+	151493220	151495220	Tnfrsf25	NM_033042
47	chr7	29517379	29517913	4	3	2.33						+	29502808	29522159	Fbxo17	NM_015796					
48	chr11	94426334	94427098	4	3	2.31	+	94425387	94427387	Chad	NM_007689	-	94419415	94462100	Acsf2	NM_153807					
49	chr5	144951705	144952579	4	3	2.31	+	144950154	144952154	Bhlha15	NM_010800										
50	chr7	25162160	25162789	4	3	2.31						+	25156281	25169231	Kcnn4	NM_008433					
51	chr8	113493856	113494415	4	3	2.31						+	113444764	113495397	St3gal2	NM_009179					

52	chr19	59541592	59542141	4	3	2.28																
53	chr8	73219028	73219977	4	3	2.28																
54	chr5	120118141	120118590	4	3	2.27																
55	chr6	52127065	52127725	4	3	2.26					-	52120060	52162066	Hoxa3	NM_010452							
56	chr14	51690831	51691475	4	3	2.25	-	51690117	51692117	Olfr750	NM_207558											
57	chr19	5745427	5746078	4	3	2.25					+	5741903	5757532	Ltbp3	NM_008520							
58	chr4	62832429	62832883	4	3	2.24	-	62832165	62834165	Kif12	NM_010616											
59	chr4	9770135	9770816	4	3	2.23																
60	chr8	73340588	73341222	4	3	2.2					+	73333347	73344322	Il12rb1	NM_008353							
61	chr8	74213328	74213678	4	3	2.2	+	74212150	74214150	Insl3	NM_013564	+	74213150	74214476	Insl3	NM_013564	+	74213476	74215476	Jak3	NM_010589	
62	chr14	67850949	67851496	4	3	2.19	+	67851128	67853128	Ebf2	NM_010095											
63	chr15	100884405	100884769	4	3	2.18																
64	chr8	3392673	3393722	4	3	2.17	+	3392007	3394007	Arhgef18	NM_133962											
65	chr15	102916892	102917246	4	3	2.14																
66	chr8	94889279	94889748	4	3	2.13																
67	chr5	123213571	123214205	4	3	2.1	-	123213303	123215303	Camkk2	NM_145358											
68	chr7	133909988	133910337	4	3	2.1	+	133908927	133910927	Gdpd3	NM_024228						+	133908330	133910330	Mapk3	NM_011952	
69	chr19	42674167	42674816	4	3	2.09					-	42667768	42686296	Loxl4	NM_053083							
70	chr12	113959508	113959867	4	3	2.08	+	113959384	113961384	AW555464	NM_001024602											
71	chr19	45082191	45083167	4	3	2.07					+	45082047	45086252	Peo1	NM_153796							
72	chr13	40830927	40831873	4	3	2.05																
73	chr17	64286974	64287742	4	3	2.05	+	64286320	64288320	Fert2	NM_008000	+	64246366	64487845	Fert2	NM_001037997						
74	chr17	23943777	23944236	4	3	2.04					+	23941153	23960710	Srrm2	NM_175229							
75	chr11	96203022	96203766	4	3	2.02					+	96185439	96208244	Hoxb3	NM_001079869							
76	chr7	13513733	13514092	4	3	2.01					+	13513764	13515421	2310014L17Ri	NM_029809							
77	chr1	91828170	91829718	4	3	2																
78	chr17	87359594	87360255	4	3	2																
79	chr1	91829957	91830765	4	3	1.99																
80	chr11	3440369	3441026	4	3	1.99																
81	chr11	96161875	96162619	4	3	1.99											+	96161883	96163883	Hoxb6	NM_008269	
82	chr6	52122404	52122953	4	3	1.98					-	52120060	52162066	Hoxa3	NM_010452							
83	chr8	73279574	73280123	4	3	1.96					+	73279577	73281585	Rab3a	NM_009001							
84	chr4	61945130	61945574	4	3	1.94																
85	chr7	25919561	25920200	4	3	1.94																
86	chr1	75418677	75419226	4	3	1.93					+	75372871	75427881	Speg	NM_007463							
87	chr11	57644744	57645698	4	3	1.93	-	57644649	57646649	Hand1	NM_008213											
88	chr15	85373911	85374485	4	3	1.93					-	85366866	85410159	Wnt7b	NM_001163633							
89	chr19	5716026	5716670	4	3	1.93					-	5708373	5725317	Ehbp1l1	NM_001114597							
90	chr4	132806851	132807700	4	3	1.92					+	132797732	132807843	Map3k6	NM_016693							
91	chr5	34669445	34670089	4	3	1.92																
92	chr5	145925933	145926392	4	3	1.91					-	145909246	145926973	Ptcd1	NM_133735							
93	chr16	48750074	48750723	4	3	1.9					-	48735802	48771069	Trat1	NM_198297							
94	chr8	73118947	73119417	4	3	1.9	+	73117379	73119379	Isyna1	NM_023627											
95	chr10	80702493	80703122	4	3	1.89					+	80696907	80713868	Zfr2	NM_001034895							
96	chr11	68369752	68370186	4	3	1.89	+	68368687	68370687	Mfsd6l	NM_146004											
97	chr11	99353894	99354540	4	3	1.89	-	99353424	99355424	Krt23	NM_033373											
98	chr18	9214145	9214900	4	3	1.89					+	9213853	9215199	Fzd8	NM_008058							
99	chr4	145930431	145930780	4	3	1.89																
100	chr5	120130396	120131020	4	3	1.89					+	120121677	120133610	Tbx3	NM_198052							
101	chr10	126518338	126519006	4	3	1.88					+	126516962	126529225	Agap2	NM_001033263							
102	chr5	98364239	98364908	4	3	1.88					-	98314706	98458981	Antxr2	NM_133738							
103	chr15	88976796	88977155	4	3	1.87					-	88973913	88979036	Mapk11	NM_011161							
104	chr7	109255243	109255902	4	3	1.87					+	109251256	109258662	Art1	NM_009710							
105	chr13	113622008	113622557	4	3	1.84					+	113591999	113656888	Ppap2a	NM_008247							
106	chr6	84085080	84085434	4	3	1.84					+	83970382	84160036	Dysf	NM_021469							
107	chr10	80785071	80785705	4	3	1.83					+	80784847	80787996	2510012J08Ril	NM_027381							
108	chr11	69672086	69672430	4	3	1.83	-	69671232	69673232	Tnk1	NM_031880											
109	chr5	125747737	125748286	4	3	1.83																
110	chr6	113432118	113432878	4	3	1.81											+	113432132	113434132	Il17rc	NM_134159	
111	chr11	48982532	48983201	4	3	1.8					-	48982826	48999591	Btnl9	NM_172793							

112	chr11	83231851	83232215	4	3	1.8					+	83224573	83233540	Rasl10b	NM_001013386							
113	chr15	61868344	61869095	4	3	1.8	+	61868541	61870541	Pvt1	NR_003368											
114	chr17	89192393	89193032	4	3	1.8																
115	chr2	103935956	103936420	4	3	1.79	+	103934957	103936957	Cd59a	NM_007652											
116	chr1	40382518	40383077	4	3	1.77					+	40382471	40421316	Il1rl2	NM_133193							
117	chr12	105847832	105848196	4	3	1.77																
118	chr5	138015644	138016293	4	3	1.77					+	138012078	138027709	Trfr2	NM_015799							
119	chr6	52193525	52193984	4	3	1.77					-	52193104	52194766	Hoxa11	NM_010450							
120	chr10	75356470	75356839	4	3	1.76	+	75355142	75357142	Derl3	NM_024440											
121	chr10	77126832	77127496	4	3	1.76																
122	chr5	143918801	143919447	4	3	1.76																
123	chr7	128535425	128535794	4	3	1.76	+	128534809	128536809	Hs3st2	NM_001081327											
124	chr9	110526657	110528026	4	3	1.76	-	110525897	110527897	Nradd	NM_026012					-	110526292	110528292	Nbeal2	NM_183276		
125	chr10	116333219	116333653	4	3	1.75	-	116332935	116334935	Gm239	NM_001033333											
126	chr16	96583690	96584131	4	3	1.75	+	96582363	96584363	Igsf5	NM_001177887											
127	chr2	32597003	32597453	4	3	1.75					+	32577591	32609514	Sh2d3c	NM_013781							
128	chr11	4963782	4964316	4	3	1.74					-	4955133	4964330	Gas2l1	NM_030228							
129	chr4	129167895	129168724	4	3	1.74	-	129167014	129169014	Tssk3	NM_080442					+	129168200	129170200	1700125D06R	NM_001085491		
130	chr8	10978379	10978933	4	3	1.74																
131	chr11	60960699	60961263	4	3	1.73										+	60960144	60962144	Tnfrsf13b	NM_021349		
132	chr19	61301742	61302176	4	3	1.72					-	61301304	61303321	Csf2ra	NM_009970							
133	chr2	119569536	119570080	4	3	1.72					+	119569072	119575989	Itpka	NM_146125							
134	chr7	135147960	135148614	4	3	1.72	+	135146891	135148891	Trim72	NM_001079932											
135	chr19	44060483	44060837	4	3	1.71	-	44060010	44062010	Cpn1	NM_030703											
136	chr17	6878031	6878675	4	3	1.7	+	6876959	6878959	Sytl3	NM_031395											
137	chr2	74541955	74542405	4	3	1.7																
138	chr8	86568369	86569219	4	3	1.7	-	86567878	86569878	Rln3	NM_173184	-	86566965	86568878	Rln3	NM_173184						
139	chr8	91549335	91549894	4	3	1.7																
140	chr12	77506795	77507149	4	3	1.69										+	77506923	77508923	Hspa2	NM_008301		
141	chr14	75536299	75536977	4	3	1.69	+	75535231	75537231	Lcp1	NM_008879											
142	chr2	174266879	174267448	4	3	1.69																
143	chr6	52152600	52153944	4	3	1.69					-	52120060	52162066	Hoxa3	NM_010452							
144	chr16	4418851	4419415	4	3	1.68	-	4418587	4420587	Adcy9	NM_009624											
145	chr18	11058953	11059322	4	3	1.68					+	11053507	11084633	Gata6	NM_010258							
146	chr4	138522868	138523532	4	3	1.68	+	138522026	138524026	Rnf186	NM_025786	+	138523026	138524281	Rnf186	NM_025786						
147	chr11	97212870	97213219	4	3	1.65	-	97212387	97214387	Gpr179	NM_001081220											
148	chr15	7087804	7088848	4	3	1.63					+	7080571	7134343	Lifr	NM_001113386							
149	chr15	77688216	77688575	4	3	1.6																
150	chr10	80852962	80853521	4	3	1.59																
151	chr11	82744784	82745543	4	3	1.59					+	82725754	82755908	Unc45b	NM_178680							
152	chr11	96163365	96164024	4	3	1.59										+	96161883	96163883	Hoxb6	NM_008269		
153	chr18	32299015	32299450	4	3	1.59	-	32298224	32300224	Proc	NM_001042767											
154	chr11	75255037	75255661	4	3	1.58										-	75253444	75255444	Wdr81	NM_138950		
155	chr11	97200028	97200677	4	3	1.58					-	97194422	97212387	Gpr179	NM_001081220							
156	chr5	138082165	138083334	4	3	1.57	+	138081700	138083700	Sap25	NM_0010819(	+	138082700	138084130	Sap25	NM_0010819(	+	138081327	138083327	Lrch4	NM_146164	
157	chr7	4098423	4098947	4	3	1.57					+	4089657	4098775	Leng8	NM_172736							
158	chr7	109007682	109008021	4	3	1.57					-	109007844	109018197	Folr1	NM_008034							
159	chr17	25608580	25609224	4	3	1.56	+	25607534	25609534	Tekt4	NM_027951											
160	chr10	79380979	79381826	4	3	1.55					+	79380715	79384017	Kiss1r	NM_053244							
161	chr11	102085857	102086501	4	3	1.55					-	102058060	102090486	Hdac5	NM_001077696							
162	chr12	9587795	9588538	4	3	1.55										+	9587306	9589306	Osr1	NM_011859		
163	chr5	72972248	72972627	4	3	1.55	-	72971323	72973323	Zar1	NM_174877					-	72971877	72973877	Gm5868	NM_001024147		
164	chr15	78267151	78267735	4	3	1.54					+	78260057	78268733	Kctd17	NM_001081367							
165	chr8	109031646	109032080	4	3	1.54																
166	chr17	28219735	28220284	4	3	1.53																
167	chr5	136344869	136345223	4	3	1.53					+	136294975	136349642	Srrm3	NM_021403							
168	chr19	6339505	6340154	4	3	1.52					+	6336038	6339894	Men1	NM_008583							
169	chr7	134507272	134507626	4	3	1.52																
170	chr9	108366319	108366881	4	3	1.52					+	108363848	108367276	Ccdc71	NM_133744							
171	chr4	151402641	151403010	4	3	1.51										-	151401022	151403022	Tas1r1	NM_031867		

172	chr9	21142296	21142740	4	3	1.51	+	21141295	21143295	Slc44a2	NM_152808										
173	chr11	120539125	120539592	4	3	1.5						+	120538974	120569760	Aspscr1	NM_198223					
174	chr14	55725914	55726479	4	3	1.49	-	55724430	55726430	Ap1g2	NM_007455						-	55724662	55726662	Jph4	NM_177049
175	chr7	128536040	128536679	4	3	1.49	+	128534809	128536809	Hs3st2	NM_001081327										
176	chr12	88222717	88223476	4	3	1.48						-	88222652	88224764	6430527G18R	NM_145836					
177	chr9	46078219	46078768	4	3	1.48						+	46077690	46079002	Apoa5	NM_080434					
178	chrX	17723126	17723660	4	3	1.47	+	17721995	17723995	Dusp21	NM_028568	+	17722995	17723818	Dusp21	NM_028568	+	17722818	17724818	Dusp21	NM_028568
179	chr15	89207616	89207960	4	3	1.46	-	89206468	89208468	Tymp	NM_138302						-	89206879	89208879	Odf3b	NM_001013022
180	chr2	152533124	152533683	4	3	1.45						+	152496196	152533404	H13	NM_010376					
181	chr9	75862664	75863098	4	3	1.45	+	75861783	75863783	Hmgcll1	NM_173731										
182	chr11	102960463	102960992	4	3	1.44						-	102932609	102961972	Plcd3	NM_152813					
183	chr6	120411547	120412424	4	3	1.44															
184	chr1	40279765	40280132	4	3	1.43															
185	chr11	3529013	3529582	4	3	1.43															
186	chr11	69840249	69840818	4	3	1.42						+	69833106	69858033	Dlg4	NM_001109752					
187	chr12	77518645	77519008	4	3	1.42	+	77517585	77519585	Gm70	NM_001163103										
188	chr19	6375542	6375909	4	3	1.42						+	6364689	6377038	Sf1	NM_011750					
189	chr11	58998288	58998969	4	3	1.41						-	58998356	59004454	Guk1	NM_008193					
190	chr15	102795536	102796106	4	3	1.41															
191	chr8	74233273	74233807	4	3	1.41						-	74233285	74248580	Fcho1	NM_028715					
192	chr6	121193470	121193729	4	3	1.4															
193	chr4	116477389	116477948	4	3	1.37						-	116477607	116479164	Toe1	NM_026654	+	116475853	116477853	Tesk2	NM_146151
194	chr17	26204546	26205095	4	3	1.36						-	26126980	26205122	Rab11fip3	NM_001162868					
195	chr4	53283766	53284030	4	3	1.36	-	53282104	53284104	AI427809	NR_033139										
196	chr7	19608063	19608413	4	3	1.35	-	19607888	19609888	Foxa3	NM_008260										
197	chr6	135014760	135015099	4	3	1.34	+	135014679	135016679	Gprc5a	NM_181444										
198	chr11	67778296	67778548	4	3	1.33	-	67778144	67780144	Wdr16	NM_027963										
199	chr2	163683863	163684212	4	3	1.33											+	163683610	163685610	Kcnk15	NM_001030292
200	chr4	146206798	146207527	4	3	1.33															
201	chr6	52114104	52114741	4	3	1.33	-	52113830	52115830	Hoxa2	NM_010451										
202	chr7	104844541	104844895	4	3	1.33	+	104844200	104846200	Clns1a	NM_023671										
203	chr7	148615000	148615449	4	3	1.33	-	148614319	148616319	Cend1	NM_021316						-	148614647	148616647	Slc25a22	NM_026646
204	chr9	107955842	107956201	4	3	1.33	+	107954489	107956489	Amigo3	NM_177275	-	107955170	107979134	Rnf123	NM_032543					
205	chr3	51199709	51200248	4	3	1.31	-	51199469	51201469	4930583H14R	NM_026358										
206	chr4	126891735	126892284	4	3	1.3						+	126847514	126913266	Dlgap3	NM_198618					
207	chr10	79353946	79354370	4	3	1.29	+	79352597	79354597	Cfd	NM_013459	+	79353597	79355401	Cfd	NM_013459					
208	chr11	69469033	69469387	4	3	1.29	+	69467874	69469874	Sox15	NM_009235	+	69468874	69470123	Sox15	NM_009235	+	69469123	69471123	Sox15	NM_009235
209	chr4	43719210	43719654	4	3	1.29	-	43718438	43720438	Olfr71	NM_019486	-	43718499	43719438	Olfr71	NM_019486	-	43717499	43719499	Olfr71	NM_019486
210	chr17	34170815	34171159	4	3	1.28						+	34169796	34174344	Rxrb	NM_011306					
211	chr9	107508011	107508365	4	3	1.27	-	107506733	107508733	Sema3b	NM_009153	-	107501445	107510572	Sema3b	NM_001042779					
212	chr1	93241043	93241507	4	3	1.26						+	93219651	93243880	Espnl	NM_001033292					
213	chr11	70429637	70430096	4	3	1.26	+	70428395	70430395	4930544D05R	NM_0011455	+	70429395	70430392	4930544D05R	NM_0011455	+	70429392	70431392	4930544D05R	NM_001145537
214	chr7	127471869	127472133	4	3	1.25	+	127471197	127473197	Abca15	NM_177213										
215	chr5	102088147	102088684	4	3	1.24											-	102087215	102089215	Nkx6-1	NM_144955
216	chr8	74203322	74203991	4	3	1.24						+	74201281	74211212	Jak3	NM_001190830					
217	chr3	88168186	88168635	4	3	1.23	+	88167510	88169510	Paqr6	NM_198410										
218	chr4	132776941	132777410	4	3	1.23	+	132775723	132777723	Cd164l2	NM_027152										
219	chr6	83037604	83038053	4	3	1.23						+	83036358	83038235	Lbx2	NM_010692	+	83037235	83039235	Lbx2	NM_010692
220	chr8	48477539	48478105	4	3	1.22															
221	chr2	77009655	77010211	4	3	1.2															
222	chr15	78857309	78857774	4	3	1.19															
223	chr9	45744003	45744265	4	3	1.19	-	45743141	45745141	Tagln	NM_011526										
224	chr15	8917861	8918631	4	3	1.18	+	8917118	8919118	Ranbp3l	NM_198024										
225	chr2	87366119	87366668	4	3	1.18															
226	chr12	115616930	115617564	4	3	1.17															
227	chr9	21860163	21860597	4	3	1.17											-	21858903	21860903	Zfp653	NM_177318
228	chr2	155834383	155835094	4	3	1.16	+	155832860	155834860	Ergic3	NM_025516										
229	chr10	81089335	81089694	4	3	1.15	-	81089067	81091067	Sirt6	NM_001163430										
230	chr13	21571118	21571477	4	3	1.14	+	21569775	21571775	Zkscan4	NM_001039115										
231	chr2	155660151	155660700	4	3	1.14	-	155659590	155661590	Fam83c	NM_027788										

232	chr1	75371737	75372421	4	3	1.13	+	75370871	75372871	Speg	NM_007463												
233	chr5	150330684	150331333	4	3	1.13	+	150330253	150332253	4930434E21Ri	NM_029440												
234	chr18	37120458	37120815	4	3	1.12	+	37119093	37121093	Pcdha5	NM_009959	+	37113394	37998854	Pcdha4-g	NM_001174154							
235	chr12	60229517	60229979	4	3	1.11	+	60229732	60231732	Ctage5	NM_146034												
236	chr2	25471539	25471983	4	3	1.11						-	25465148	25472198	4921530D09R	NM_029859							
237	chr4	46633206	46633755	4	3	1.11						-	46618261	46662071	Tbc1d2	NM_198664							
238	chr9	21992578	21992937	4	3	1.11	+	21991609	21993609	Zfp872	NM_001033813												
239	chr11	78155193	78155442	4	3	1.1											+	78155278	78157278	Pigs	NM_201406		
240	chr17	34732190	34732724	4	3	1.1						+	34730415	34733286	Pbx2	NM_017463							
241	chr2	118536698	118537252	4	3	1.09						-	118534252	118553174	Plcb2	NM_177568							
242	chr3	84756019	84756348	4	3	1.08	+	84755132	84757132	Fbxw7	NM_080428	+	84669066	84782120	Fbxw7	NM_001177774							
243	chr2	127366936	127367380	4	3	1.07	-	127366153	127368153	Prom2	NM_178047												
244	chr19	33466381	33467047	4	3	1.06	-	33465785	33467785	Rnls	NM_001146342												
245	chr18	37249925	37250374	4	3	1.05	+	37248789	37250789	Pcdhac1	NM_00100367	+	37113394	37998854	Pcdha4-g	NM_001174154							
246	chr10	58866537	58867021	4	3	1.04	+	58865432	58867432	Pla2g12b	NM_023530												
247	chr19	37769766	37770232	4	3	1.04																	
248	chr4	135051733	135052167	4	3	1.04	+	135050901	135052901	4930555I21Ril	NM_030189												
249	chrX	137212743	137213092	4	3	1.04	+	137211566	137213566	Mid2	NM_011845												
250	chr19	38207421	38208061	4	3	1.02	+	38206270	38208270	Pde6c	NM_001170959												
251	chr11	115119073	115119532	4	3	1.01						-	115111482	115127557	Grin2c	NM_010350							

T0 vs C

	chr	start	end	NCaseV	NContrc	caseVScontrol	prc	promoter.Star	promoter.End	promoter.Sym	promoter.Acc	intr	intragenic.Star	intragenic.End	intragenic.Sym	intragenic.Acc	dov	downstream.S	downstream.E	downstream.S	downstream.Accession
1	chr11	96207041	96207580	4	3	2.77						+	96185439	96208244	Hoxb3	NM_001079869					
2	chr11	96205391	96205930	4	3	2.5	+	96204082	96206082	Hoxb3	NM_010458	+	96185439	96208244	Hoxb3	NM_001079869					
3	chr11	49447570	49447999	4	3	2.17						+	49424180	49465241	Flt4	NM_008029					
4	chr1	186551383	186552042	4	3	2.1											-	186550023	186552023	Hlx	NM_008250
5	chr11	96166037	96166716	4	3	2.02						+	96165825	96166435	Hoxb5	NM_008268					
6	chr17	39982837	39983271	4	3	2.02															
7	chr11	85654095	85654664	4	3	1.92						+	85647116	85654450	Tbx2	NM_009324					
8	chr2	9796191	9796665	4	3	1.88						-	9779704	9799227	Gata3	NM_008091					
9	chr11	96203127	96203666	4	3	1.86						+	96185439	96208244	Hoxb3	NM_001079869					
10	chr1	91830182	91830562	4	3	1.84															
11	chr11	98797428	98797777	4	3	1.84															
12	chr9	55393284	55393838	4	3	1.83											+	55392985	55394985	Isl2	NM_027397
13	chr8	3392778	3393622	4	3	1.77	+	3392007	3394007	Arhgef18	NM_133962										
14	chr6	125031667	125032316	4	3	1.73											+	125031490	125033490	Lpar5	NM_001163268
15	chr7	31018357	31018806	4	3	1.72											+	31017406	31019406	Polr2i	NM_027259
16	chr9	21116550	21116989	4	3	1.7	-	21115777	21117777	Ap1m2	NM_001110300										
17	chr12	110697768	110698417	4	3	1.67						+	110692664	110700546	Dlk1	NM_001190703					
18	chr7	109255548	109255902	4	3	1.65						+	109251256	109258662	Art1	NM_009710					
19	chr17	56095452	56095976	4	3	1.62											+	56095445	56097445	Ebi3	NM_015766
20	chr13	55515975	55516509	4	3	1.61	-	55515593	55517593	Pfn3	NM_029303	-	55516048	55516593	Pfn3	NM_029303	-	55515048	55517048	Pfn3	NM_029303
21	chr11	96164790	96165515	4	3	1.59	+	96163825	96165825	Hoxb5	NM_008268										
22	chr11	97659443	97659897	4	3	1.57															
23	chr7	25919561	25920095	4	3	1.57															
24	chr9	106787364	106788013	4	3	1.53						-	106787315	106788331	Rbm15b	NM_175402					
25	chr16	17804364	17804813	4	3	1.52						+	17798374	17807380	Scarf2	NM_153790					
26	chr2	74530379	74530838	4	3	1.5	+	74529004	74531004	Hoxd10	NM_013554										
27	chr6	52127065	52127725	4	3	1.49						-	52120060	52162066	Hoxa3	NM_010452					
28	chr16	48750074	48750723	4	3	1.48						-	48735802	48771069	Trat1	NM_198297					
29	chr5	125747737	125748286	4	3	1.47															
30	chr10	126763689	126764051	4	3	1.46						+	126761782	126765999	Arhgap9	NM_146011					
31	chr9	21992578	21993130	4	3	1.45	+	21991609	21993609	Zfp872	NM_001033813										
32	chr8	73119047	73119417	4	3	1.44	+	73117379	73119379	Isyna1	NM_023627										
33	chr8	73340673	73341222	4	3	1.42						+	73333347	73344322	Il12rb1	NM_008353					
34	chr3	88340120	88340454	4	3	1.39	-	88339304	88341304	Mir1905	NR_035434	+	88337316	88344316	Mex3a	NM_00102985	-	88339222	88341222	Mir1905	NR_035434
35	chr4	116477499	116477948	4	3	1.36						-	116477607	116479164	Toe1	NM_026654	+	116475853	116477853	Tesk2	NM_146151

36	chr17	46785124	46785563	4	3	1.35						+	46784196	46786081	Mrpl2	NM_025302					
37	chr11	97200318	97200577	4	3	1.33						-	97194422	97212387	Gpr179	NM_001081220					
38	chr5	144049361	144049805	4	3	1.31															
39	chr3	96488547	96489208	4	3	1.29						+	96475053	96493957	Ankrd35	NM_001081139					
40	chr5	135752281	135752733	4	3	1.25															
41	chr6	5145623	5146072	4	3	1.24															
42	chr7	4098423	4098947	4	3	1.24						+	4089657	4098775	Leng8	NM_172736					
43	chr10	80785071	80785705	4	3	1.23						+	80784847	80787996	2510012J08Ril	NM_027381					
44	chr8	73279674	73280033	4	3	1.22						+	73279577	73281585	Rab3a	NM_009001					
45	chr9	46078219	46078643	4	3	1.22						+	46077690	46079002	Apoa5	NM_080434					
46	chr11	98247933	98248391	4	3	1.2	+	98246945	98248945	Pnmt	NM_008890	+	98247945	98249411	Pnmt	NM_008890					
47	chr12	3235435	3235992	4	3	1.19	+	3234790	3236790	1700012B15Ri	NR_015551										
48	chr5	144951910	144952344	4	3	1.19	+	144950154	144952154	Bhlha15	NM_010800										
49	chr8	86568574	86569033	4	3	1.19	-	86567878	86569878	Rln3	NM_173184	-	86566965	86568878	Rln3	NM_173184					
50	chr10	77126947	77127296	4	3	1.15															
51	chr17	13292035	13292443	4	3	1.15	-	13290338	13292338	Gm11166	NR_024558	+	13255056	13568627	Tcp10a	NM_009340					
52	chr17	34808092	34808726	4	3	1.15	+	34806479	34808479	Tnxb	NM_031176										
53	chr3	83994590	83994939	4	3	1.13						-	83966795	84023799	Trim2	NM_030706					
54	chr15	80502642	80502911	4	3	1.11	+	80501276	80503276	Fam83f	NM_145986										
55	chr16	31317171	31317547	4	3	1.11															
56	chr19	45082511	45082984	4	3	1.1						+	45082047	45086252	Peo1	NM_153796					
57	chr6	52152500	52153529	4	3	1.1						-	52120060	52162066	Hoxa3	NM_010452					
58	chr7	5010940	5011379	4	3	1.1						+	5009327	5011386	Ccdc106	NM_146178					
59	chr17	34732190	34732939	4	3	1.04						+	34730415	34733286	Pbx2	NM_017463					
60	chr11	110115505	110115982	4	3	1.03															

Hypomethylated CGIs

T2 vs C

	chr	start	end	NCaseV	NContr	caseVScontrol	pr	promoter.Star	promoter.End	promoter.Sym	promoter.Acc	intr	intragenic.Star	intragenic.End	intragenic.Sym	intragenic.Acc	dov	downstream.S	downstream.E	downstream.S	downstream.Accession
1	chr6	145069530	145070029	3	4	3.11	+	145069258	145071258	Lrmp	NM_008511										
2	chr5	28785345	28785704	3	4	2.97						-	28784379	28792641	Shh	NM_009170					
3	chr19	44910787	44911211	3	4	2.61											+	44909517	44911517	Pax2	NM_011037
4	chr1	189431182	189431548	3	4	2.49															
5	chr3	145315156	145315505	3	4	2.3															
6	chr9	15514038	15514999	3	4	2.11	+	15513212	15515212	Slc36a4	NM_172289										
7	chr11	97395992	97396431	3	4	2.02						-	97371653	97435440	Srcin1	NM_018873					
8	chr2	69218384	69218738	3	4	2.02	+	69217518	69219518	Dhrs9	NM_175512										
9	chr11	53279913	53280372	3	4	1.89						+	53271706	53280257	Shroom1	NM_027917					
10	chr2	62411748	62412097	3	4	1.61	-	62411078	62413078	Fap	NM_007986										
11	chr15	85406831	85407584	3	4	1.6						-	85366866	85410159	Wnt7b	NM_001163633					
12	chr12	75009296	75009752	3	4	1.59	+	75007853	75009853	Hif1a	NM_010431										
13	chr7	106616944	106617383	3	4	1.58						+	106615513	106621530	Klhl35	NM_028145					
14	chr11	68198738	68199087	3	4	1.5						-	68023865	68199328	Ntn1	NM_008744					
15	chr1	74830695	74831044	3	4	1.48						+	74819465	74830893	Wnt6	NM_009526					
16	chr11	100275654	100276013	3	4	1.43	-	100275133	100277133	1110036O03R	NM_176830										
17	chr15	78744399	78744853	3	4	1.43	+	78743348	78745348	Pdxp	NM_020271										
18	chr19	24248440	24248887	3	4	1.42						-	24169991	24298444	Tjp2	NM_011597					
19	chr15	84686136	84686485	3	4	1.4	-	84685559	84687559	Phf21b	NM_001081166										
20	chr5	23857305	23857654	3	4	1.4	-	23856422	23858422	Kcnh2	NM_013569										
21	chr8	90723100	90723454	3	4	1.34	+	90722111	90724111	Papd5	NM_001164497										
22	chr2	73613240	73613589	3	4	1.33	-	73612403	73614403	Chn1	NM_001113246										
23	chr7	13609687	13610317	3	4	1.33	+	13608500	13610500	Trim28	NM_011588										
24	chrX	39502072	39502506	3	4	1.32	+	39501588	39503588	Stag2	NM_001077712										
25	chr11	23533395	23533744	3	4	1.3	-	23532631	23534631	0610010F05Ri	NM_027860										
26	chr7	29079459	29079903	3	4	1.3						-	29079573	29085804	Dll3	NM_007866					
27	chr11	116273925	116274369	3	4	1.29	-	116273346	116275346	Rnf157	NM_027258										
28	chr1	182571553	182571883	3	4	1.28	+	182570464	182572464	Lin9	NM_175186										

29	chr10	92623450	92623801	3	4	1.28	+	92622620	92624620	Cdk17	NM_146239									
30	chr8	94984419	94984848	3	4	1.28														
31	chr4	100449306	100449671	3	4	1.26	+	100448283	100450283	Cachd1	NM_198037									
32	chr8	86521752	86522288	3	4	1.26	+	86520570	86522570	Samd1	NM_001081415									
33	chr11	104303386	104303915	3	4	1.25	-	104302605	104304605	1700081L11Ri	NM_001081045									
34	chr12	112615753	112616197	3	4	1.24	-	112614929	112616929	Cdc42bpb	NM_183016									
35	chr13	58229736	58230399	3	4	1.24	-	58228917	58230917	Hnrnpa0	NM_029872									
36	chr16	77014053	77014412	3	4	1.24	+	77013313	77015313	Usp25	NM_013918									
37	chr17	31992630	31992983	3	4	1.24	-	31991737	31993737	Sik1	NM_010831									
38	chr9	51856357	51856811	3	4	1.24	+	51855045	51857045	Rdx	NM_00110461	+	51856254	51895843	Rdx	NM_001104616				
39	chr1	79855007	79855468	3	4	1.23	-	79854240	79856240	Serpine2	NM_009255									
40	chr2	3391942	3392381	3	4	1.22	-	3391258	3393258	Suv39h2	NM_022724									
41	chr5	34630959	34631308	3	4	1.22	-	34629973	34631973	Zfyve28	NM_001015039									
42	chr6	72047583	72048022	3	4	1.22	+	72046606	72048606	St3gal5	NM_011375									
43	chr11	4961494	4961748	3	4	1.21						-	4955133	4964330	Gas2l1	NM_030228				
44	chr19	41921986	41922455	3	4	1.21	-	41921622	41923622	Frat2	NM_177603									
45	chr3	121996168	121996637	3	4	1.21	-	121995621	121997621	Mir760	NR_030439						-	121995502	121997502	Mir760	NR_030439
46	chr5	50449903	50450362	3	4	1.21	-	50449235	50451235	Gpr125	NM_133911									
47	chr8	119681885	119682234	3	4	1.21	+	119681034	119683034	Gan	NM_001081151									
48	chr1	91864838	91865192	3	4	1.2						-	91850252	91910152	Asb18	NM_139152				
49	chr6	90938042	90938471	3	4	1.2														
50	chr10	81007664	81008071	3	4	1.19	-	81006791	81008791	Gna11	NM_010301									
51	chr11	54679903	54680477	3	4	1.19	+	54678939	54680939	Hint1	NM_008248									
52	chr17	24625367	24625916	3	4	1.19	+	24624727	24626727	Caskin1	NM_027937									
53	chr4	128561354	128561613	3	4	1.19	+	128560383	128562383	Trim62	NM_178110									
54	chr7	144505319	144505985	3	4	1.19	-	144505128	144507128	Ebf3	NM_010096									
55	chr12	109513150	109513584	3	4	1.18	-	109512627	109514627	Ccdc85c	NM_001159910									
56	chr17	81127316	81127665	3	4	1.18	-	81126433	81128433	Map4k3	NM_001081357									
57	chr19	6364087	6364551	3	4	1.18	+	6362689	6364689	Sf1	NM_011750									
58	chr4	151235330	151235686	3	4	1.18	-	151234866	151236866	Camta1	NM_001166021									
59	chr6	92041715	92042089	3	4	1.18	+	92040411	92042411	Nr2c2	NM_011630									
60	chr1	134942579	134943008	3	4	1.17	+	134941588	134943588	Pik3c2b	NM_001099276									
61	chr4	21615970	21616419	3	4	1.17														
62	chr6	56747170	56747638	3	4	1.17	-	56746807	56748807	Kbtbd2	NM_145958									
63	chr7	71083454	71083916	3	4	1.17	-	71082801	71084801	Klf13	NM_021366									
64	chr10	60294100	60294364	3	4	1.16	-	60293329	60295329	Unc5b	NM_029770									
65	chr1	194681117	194681810	3	4	1.15	-	194680946	194682946	Sertad4	NM_198247									
66	chr14	65880563	65881032	3	4	1.15	-	65880300	65882300	Fzd3	NM_021458									
67	chr17	24686991	24687355	3	4	1.15	+	24685894	24687894	Pkd1	NM_013630									
68	chr2	158235529	158235788	3	4	1.15	+	158234588	158236588	Ralgapb	NM_177658									
69	chr7	70589788	70590232	3	4	1.15	+	70588657	70590657	Otud7a	NM_130880									
70	chr7	88851441	88851810	3	4	1.15	-	88850811	88852811	Homer2	NM_001164086									
71	chr17	53706359	53706752	3	4	1.14	+	53705295	53707295	Kat2b	NM_020005									
72	chr8	108160392	108160830	3	4	1.14	+	108159437	108161437	Ctcf	NM_181322									
73	chr11	32121975	32122424	3	4	1.13	-	32121293	32123293	Rhbdf1	NM_010117									
74	chr15	85036261	85036623	3	4	1.13	+	85035437	85037437	Fbln1	NM_010180									
75	chr5	111846327	111846796	3	4	1.13	+	111846185	111848185	Mn1	NM_001081235									
76	chr9	75458703	75459062	3	4	1.13	-	75458132	75460132	Tmod2	NM_016711									
77	chr9	95459855	95460235	3	4	1.13	+	95459235	95461235	Paqr9	NM_198414									
78	chr1	36569111	36569660	3	4	1.12	+	36567720	36569720	Cnnm3	NM_053186									
79	chr4	136833416	136833788	3	4	1.12	+	136832549	136834549	Wnt4	NM_009523									
80	chr5	37086978	37087332	3	4	1.12	-	37086208	37088208	D5Ertd579e	NM_001081232									
81	chr13	60277311	60278065	3	4	1.11						-	60276765	60277896	Gas1	NM_008086				
82	chr16	94511477	94511846	3	4	1.11														
83	chr11	69153940	69154289	3	4	1.1	+	69153270	69155270	A030009H04R	NR_027827									
84	chr12	70284760	70285215	3	4	1.1	+	70284144	70286144	Mgat2	NM_146035	-	70283720	70285054	Rpl36al	NM_025589				
85	chr13	15555811	15556250	3	4	1.09	+	15554555	15556555	Gli3	NM_008130									
86	chr8	97056618	97057087	3	4	1.09	+	97055927	97057927	Cpne2	NM_153507									
87	chr1	6204910	6205269	3	4	1.08	+	6203742	6205742	Rb1cc1	NM_009826									
88	chr1	91476844	91477378	3	4	1.08						+	91352385	91790857	Agap1	NM_178119				

89	chr13	53076261	53076715	3	4	1.08	-	53075408	53077408	Nfil3	NM_017373											
90	chr15	53177502	53178071	3	4	1.08	-	53176738	53178738	Ext1	NM_010162											
91	chr9	86358189	86358633	3	4	1.08	-	86357523	86359523	Ube2cbp	NM_027394											
92	chr17	15841843	15842397	3	4	1.07	+	15840930	15842930	Chd1	NM_007690											
93	chr5	17865913	17866362	3	4	1.07	-	17865231	17867231	Gnai1	NM_010305											
94	chr6	146836925	146837278	3	4	1.07	+	146836015	146838015	Ppfibp1	NM_001170433											
95	chr8	128998336	128998980	3	4	1.07	-	128997965	128999965	Tarbp1	NM_001159907											
96	chr12	112950942	112951571	3	4	1.06	+	112950479	112952479	2810002N01R	NM_001163388											
97	chr16	18877241	18877598	3	4	1.06	-	18875730	18877730	Mrpl40	NM_010922											
98	chr4	33118126	33118785	3	4	1.06	+	33117399	33119399	Ube2j1	NM_019586											
99	chr4	57312692	57313123	3	4	1.06						-	57204712	57313709	Ptpn3	NM_011207						
100	chr4	137149860	137150299	3	4	1.06	+	137149103	137151103	Usp48	NM_130879											
101	chr4	154229974	154230343	3	4	1.06	+	154229308	154231308	Ttc34	NM_172878											
102	chr1	158869283	158869952	3	4	1.05	-	158868518	158870518	Ralgps2	NM_001159966											
103	chr11	62352318	62352670	3	4	1.05	-	62351763	62353763	Cenpv	NM_028448											
104	chr13	54398063	54398515	3	4	1.04																
105	chr6	28782210	28782960	3	4	1.04	-	28780747	28782747	Lrrc4	NM_138682	+	28431347	28837832	Snd1	NM_019776						
106	chr1	39592602	39593136	3	4	1.03	+	39591646	39593646	D1Bwg0212e	NM_028043											
107	chr11	117516003	117516541	3	4	1.03	+	117514602	117516602	Tnrc6c	NM_198022											
108	chr15	93166544	93167083	3	4	1.03	-	93166366	93168366	Yaf2	NM_024189											
109	chr17	46434788	46435058	3	4	1.03	+	46433369	46435369	Dlk2	NM_207666											
110	chr18	80904545	80904899	3	4	1.03	-	80903912	80905912	Nfatc1	NM_0011641	-	80803943	80908810	Nfatc1	NM_198429						
111	chr19	40905467	40906211	3	4	1.03	+	40904768	40906768	Ccnj	NM_172839											
112	chr3	8667098	8667472	3	4	1.03	-	8666038	8668038	Hey1	NM_010423											
113	chr8	41597150	41597594	3	4	1.03	+	41596136	41598136	Vps37a	NM_033560											
114	chr1	90598451	90598890	3	4	1.02	-	90597766	90599766	Arl4c	NM_177305											
115	chr11	97049292	97049741	3	4	1.02	-	97048206	97050206	Kpnb1	NM_008379											
116	chr12	81619830	81620190	3	4	1.02	+	81618976	81620976	Galntl1	NM_001081421											
117	chr14	55495262	55495906	3	4	1.02	-	55495375	55497375	Ppp1r3e	NM_0011679(	-	55494433	55496375	Ppp1r3e	NM_001167908						
118	chr10	116387105	116387459	3	4	1.01	-	116386436	116388436	Rab3ip	NM_001003950											
119	chr11	20991524	20991773	3	4	1.01	+	20990326	20992326	Peli1	NM_023324											
120	chr4	45543281	45543730	3	4	1.01	-	45542700	45544700	Shb	NM_001033306											
121	chr12	112277610	112278165	3	4	1	+	112277008	112279008	Rcor1	NM_198023											

T0 vs C

	chr	start	end	NCaseV	NContrc	caseVScontrol	prc	promoter.Star	promoter.End	promoter.Sym	promoter.Acc	intr	intragenic.Star	intragenic.End	intragenic.Sym	intragenic.Acc	dov	downstream.S	downstream.E	downstream.S	downstream.Accession
1	chr1	6204910	6205269	3	4	1.02	+	6203742	6205742	Rb1cc1	NM_009826										
2	chr1	79855007	79855468	3	4	1.05	-	79854240	79856240	Serpine2	NM_009255										
3	chr1	182571553	182571883	3	4	1.17	+	182570464	182572464	Lin9	NM_175186										
4	chr10	81007664	81008071	3	4	1.12	-	81006791	81008791	Gna11	NM_010301										
5	chr10	92623450	92623801	3	4	1.19	+	92622620	92624620	Cdk17	NM_146239										
6	chr11	4961494	4961748	3	4	1.06						-	4955133	4964330	Gas2l1	NM_030228					
7	chr11	23533395	23533744	3	4	1.1	-	23532631	23534631	0610010F05Ri	NM_027860										
8	chr11	54679903	54680477	3	4	1.12	+	54678939	54680939	Hint1	NM_008248										
9	chr11	68198738	68199087	3	4	1.19						-	68023865	68199328	Ntn1	NM_008744					
10	chr11	69153940	69154289	3	4	1.01	+	69153270	69155270	A030009H04R	NR_027827										
11	chr11	100275654	100276013	3	4	1.01	-	100275133	100277133	1110036O03R	NM_176830										
12	chr11	104303386	104303915	3	4	1.09	-	104302605	104304605	1700081L11Ri	NM_001081045										
13	chr11	120098402	120098751	3	4	1.03						+	120095260	120152611	Bahcc1	NM_198423					
14	chr12	17999573	17999929	3	4	1.36															
15	chr12	75009296	75009752	3	4	1.38	+	75007853	75009853	Hif1a	NM_010431										
16	chr12	109513150	109513584	3	4	1.18	-	109512627	109514627	Ccdc85c	NM_001159910										
17	chr12	112615753	112616197	3	4	1.17	-	112614929	112616929	Cdc42bpb	NM_183016										
18	chr13	53076261	53076715	3	4	1.01	-	53075408	53077408	Nfil3	NM_017373										
19	chr13	58229736	58230399	3	4	1.26	-	58228917	58230917	Hnrnpa0	NM_029872										
20	chr13	60277311	60278065	3	4	1.03						-	60276765	60277896	Gas1	NM_008086					
21	chr13	101386684	101387119	3	4	1.01	-	101385926	101387926	Marveld2	NM_001038602						-	101386118	101388118	Rad17	NM_001044371
22	chr13	108679645	108680134	3	4	1.26	-	108679258	108681258	Zswim6	NM_145456										

23	chr14	35123896	35124250	3	4	1.15	+	35122912	35124912	Glud1	NM_008133											
24	chr14	65880563	65881032	3	4	1.06	-	65880300	65882300	Fzd3	NM_021458											
25	chr14	115440982	115441347	3	4	1.26																
26	chr15	53177502	53178071	3	4	1.02	-	53176738	53178738	Ext1	NM_010162											
27	chr15	84686136	84686485	3	4	1.32	-	84685559	84687559	Phf21b	NM_001081166											
28	chr17	15841843	15842397	3	4	1.03	+	15840930	15842930	Chd1	NM_007690											
29	chr17	24686991	24687355	3	4	1.13	+	24685894	24687894	Pkd1	NM_013630											
30	chr17	80772534	80772883	3	4	1.15	-	80771882	80773882	Gm10190	NR_028385	+	80707746	80787029	Arhgef33	NM_001145452						
31	chr17	81127316	81127665	3	4	1.18	-	81126433	81128433	Map4k3	NM_001081357											
32	chr17	87507029	87507379	3	4	1.09	+	87506018	87508018	Socs5	NM_019654											
33	chr19	6364087	6364551	3	4	1.07	+	6362689	6364689	Sf1	NM_011750											
34	chr19	24248440	24248887	3	4	1.3						-	24169991	24298444	Tjp2	NM_011597						
35	chr19	41921986	41922455	3	4	1.2	-	41921622	41923622	Frat2	NM_177603											
36	chr2	61649722	61650266	3	4	1.09						+	61643509	61651170	Tbr1	NM_009322						
37	chr2	73613240	73613589	3	4	1.28	-	73612403	73614403	Chn1	NM_001113246											
38	chr2	146909798	146910227	3	4	1.04						-	146909611	146911081	Nkx2-4	NM_023504	-	146908611	146910611	Nkx2-4	NM_023504	
39	chr3	121996168	121996637	3	4	1.03	-	121995621	121997621	Mir760	NR_030439						-	121995502	121997502	Mir760	NR_030439	
40	chr4	128561354	128561613	3	4	1.06	+	128560383	128562383	Trim62	NM_178110											
41	chr4	136833416	136833788	3	4	1.15	+	136832549	136834549	Wnt4	NM_009523											
42	chr4	137149860	137150299	3	4	1.01	+	137149103	137151103	Usp48	NM_130879											
43	chr4	151235330	151235686	3	4	1.04	-	151234866	151236866	Camta1	NM_001166021											
44	chr5	23857305	23857654	3	4	1.15	-	23856422	23858422	Kcnh2	NM_013569											
45	chr5	34630959	34631308	3	4	1.31	-	34629973	34631973	Zfyve28	NM_001015039											
46	chr5	37086978	37087332	3	4	1.04	-	37086208	37088208	D5Ertd579e	NM_001081232											
47	chr5	50449903	50450362	3	4	1.1	-	50449235	50451235	Gpr125	NM_133911											
48	chr6	90938042	90938471	3	4	1.28																
49	chr6	92041715	92042089	3	4	1.2	+	92040411	92042411	Nr2c2	NM_011630											
50	chr6	99643040	99643304	3	4	1.03	+	99641672	99643672	Gpr27	NM_008158	+	99642672	99643812	Gpr27	NM_008158	+	99642812	99644812	Gpr27	NM_008158	
51	chr7	13609687	13610317	3	4	1.08	+	13608500	13610500	Trim28	NM_011588											
52	chr7	17471136	17471693	3	4	1.12						+	17461665	17471650	Dact3	NM_001081655						
53	chr7	29079459	29079903	3	4	1.18						-	29079573	29085804	Dll3	NM_007866						
54	chr7	35098222	35098571	3	4	1.24																
55	chr7	69608973	69609442	3	4	1.3	-	69608396	69610396	Peg12	NM_013788											
56	chr8	86521752	86522288	3	4	1.11	+	86520570	86522570	Samd1	NM_001081415											
57	chr8	87083228	87083582	3	4	1.07						+	86940262	87163148	Cacna1a	NM_007578						
58	chr8	90723100	90723454	3	4	1.26	+	90722111	90724111	Papd5	NM_001164497											
59	chr8	97056618	97057087	3	4	1.01	+	97055927	97057927	Cpne2	NM_153507											
60	chr9	55130710	55131077	3	4	1.16	-	55130432	55132432	Nrg4	NM_032002											
61	chr9	75458703	75459062	3	4	1.11	-	75458132	75460132	Tmod2	NM_016711											
62	chr9	86358189	86358633	3	4	1.08	-	86357523	86359523	Ube2cbp	NM_027394											
63	chrX	39502072	39502506	3	4	1.05	+	39501588	39503588	Stag2	NM_001077712											